RAFAEL AFONSO DO NASCIMENTO REIS

AVALIAÇÃO DA DENSIDADE SUPERFICIAL DO MAR E CONTEÚDO DE CALOR OCEÂNICO NO OCEANO AUSTRAL A PARTIR DE DADOS DE REANÁLISE

Tese apresentada à Universidade Federal de Viçosa, como parte das exigências do Programa de Pós-Graduação em Meteorologia Aplicada, para obtenção do título de *Doctor Scientiae*.

Orientador: Flávio Barbosa Justino

Coorientador: Luís Felipe Ferreira de Mendonça

VIÇOSA - MINAS GERAIS
2022

Ficha catalográfica elaborada pela Biblioteca Central da Universidade Federal de Viçosa - Campus Viçosa

T
R375a
2022

Reis, Rafael Afonso do Nascimento, 1989-
Avaliação da densidade superficial do mar e do conteúdo de calor oceânico no Oceano Austral a partir de dados de reanálises / Rafael Afonso do Nascimento Reis. – Viçosa, MG, 2022.
1 tese eletrônica (74 f.): il. (algumas color.).

Orientador: Flávio Barbosa Justino.
Tese (doutorado) - Universidade Federal de Viçosa, Departamento de Engenharia Agrícola, 2022.
Inclui bibliografia.
DOI: https://doi.org/10.47328/ufvbbt.2022.149
Modo de acesso: World Wide Web.

1. Oceanografia - Métodos estatísticos. 2. Interação oceano-atmosfera. 3. El Niño Oscilação Sul. 4. Oceano - Temperatura. 5. Salinidade. I. Justino, Flávio Barbosa, 1971-. II. Universidade Federal de Viçosa. Departamento de Engenharia Agrícola. Programa de Pós-Graduação em Meteorologia Aplicada. III. Título.

CDD 22. ed. 551.46217

Bibliotecário(a) responsável: Renata de Fátima Alves CRB6/2578

RAFAEL AFONSO DO NASCIMENTO REIS

AVALIAÇÃO DA DENSIDADE SUPERFICIAL DO MAR E DO CONTEÚDO DE CALOR OCEÂNICO NO OCEANO AUSTRAL A PARTIR DE DADOS DE REANÁLISES

Tese apresentada à Universidade Federal de Viçosa, como parte das exigências do Programa de Pós-Graduação em Meteorologia Aplicada, para obtenção do título de *Doctor Scientiae*.

APROVADA: 20 de janeiro de 2022.

Assentimento:

Rafael Afonso do Nascimento Reis
Autor

Flávio Barbosa Justino
Orientador

À minha família, tanto a em que nasci quanto a
que escolhi para chamar de família.

AGRADECIMENTOS

À minha família: ao seu Jairo (também conhecido como meu pai), à dona Mirna (também conhecida como minha mãe) e ao meu "ermão" Matheus, por todo apoio e suporte durante toda minha vida e, em especial, neste período estressante e louco chamado doutorado.

Aos meus amigos de Santa Maria (William, Igor e Victor), por entenderem que eu não poderia estar sempre presente, mas, mesmo à distância, me ajudaram imensamente.

À Gabriela Azevedo, por todo apoio, incentivo e ajuda durante todo o tempo e por sempre acreditar em mim.

Aos amigos que fiz em Viçosa (muitos para mencionar individualmente), pelos momentos de descontração e apoio durante todos esses anos.

Aos meus orientadores, os doutores Flávio Justino e Luís Felipe Mendonça, por toda ajuda e paciência.

Ao Programa de Pós-Graduação em Meteorologia Aplicada, pela oportunidade de realizar o doutorado e, em especial, ao anjo que existe na pós, Graça Freitas, a quem eu devo muito por toda a paciência e ajuda nesses anos de curso.

O presente trabalho foi realizado com apoio da Coordenação de Aperfeiçoamento de Pessoal de Nível Superior – Brasil (CAPES) – Código de Financiamento 001.

À Fundação de Amparo à Pesquisa do Estado de Minas Gerais (FAPEMIG), pela concessão da bolsa de estudos durante o primeiro ano de curso.

À Coordenação de Aperfeiçoamento de Pessoal de Nível Superior (CAPES), pela concessão da bolsa de estudos durante os anos seguintes.

“Do or do not, there is no try”.
(Master Yoda)

RESUMO

REIS, Rafael Afonso do Nascimento, D.Sc., Universidade Federal de Viçosa, janeiro de 2022. **Avaliação da densidade superficial do mar e conteúdo de calor oceânico no Oceano Austral**. Orientador: Flávio Barbosa Justino. Coorientador: Luís Felipe Ferreira de Mendonça.

O Oceano Austral é uma peça-chave do clima global. Ele sozinho é responsável pela maior parte do sequestro de dióxido de carbono e calor antropogênico. Apesar de sua importância, ele permanece pobremente amostrado e muitos estudos visam a utilização de reanalises e modelos oceânicos para melhor compreender este tão importante oceano. Com base nisso, este trabalho estuda a capacidade das reanálises GLORYS, ORAS5 e GODAS em representarem a densidade neutra em superfície e o conteúdo de calor na camada de 0 a 300 metros do Oceano Austral. As reanálises apresentam erro na densidade neutra em relação aos dados coletados in situ, variando entre -1 e 2 kg/m³. A maior parte dos erros significativos ocorre na década de 1990 em virtude da baixa cobertura de dados de sensoriamento remoto da região. As tendências de densidade neutra das reanálises são distintas, devido aos diferentes perfis de salinidade. Todas as reanálises apresentam perfis de tendência de temperatura e de fluxos de densidade muito similares. O ORAS5 é o mais diferente entre as reanálises, pois apresenta uma tendência negativa de salinidade e de densidade neutra para a maioria do Oceano Austral. Acredita-se que o motivo dessa tendência é o fato de sua salinidade ser restringida por um processo chamado *nudging*. Em relação ao conteúdo de calor, todas as reanálises apresentam crescimento do conteúdo de calor, sendo o mais intenso o GLORYS com um aumento de $1{,}38 \times 10^{18}$ J/yr. O primeiro módulo de variabilidade das reanálises é diretamente ligado ao ENOS com GLORYS e ORAS5 apresentando uma correlação maior que GODAS e tendo um claro Dipolo Antártico. O segundo modo de variabilidade é representado por GLORYS e ORAS5, por estar relacionado aos vórtices oceânicos, cuja reanálise GODAS não resolve. GLORYS e ORAS5 são as únicas a apresentarem correlação com a MAS. A MAS impacta o conteúdo de calor também com um Dipolo Antártico, mas de maneira contrária ao ENOS. Ao se retirar o sinal do ENOS da correlação da MAS com o conteúdo de calor, é possível verificar que ela perde a característica de dipolo. Isso indica que a MAS age mais como um regular do impacto do ENOS do que por si própria no Oceano Austral. Os dois modelos oceânicos MOM025 e MOM, rodados com os parâmetros do experimento CORE-II, falham em representar o conteúdo de calor no Oceano

Austral; bem como seus módulos de variabilidade em razão de eles descartarem o impacto do ENOS no conteúdo de calor.

Palavras-chave: GODAS. GLORYS. ORAS5. ENSO. SAM. Salinidade na superfície do mar. Fluxos de densidade. CORE-II.

ABSTRACT

REIS, Rafael Afonso do Nascimento, D.Sc., Universidade Federal de Viçosa, January, 2022. **Assessment of sea surface density and ocean heat content in the Southern Ocean**. Adviser: Flávio Barbosa Justino. Co-adviser: Luís Felipe Ferreira de Mendonça.

The Southern Ocean is a key part of the global climate. It alone is responsible for most of the carbon dioxide and anthropogenic heat uptake. However, despite its importance, it remains poorly sampled and many studies aim to use reanalysis and ocean models to better understand this so important ocean. In view of this, this work studies the capabilities of the GLORYS, ORAS5 and GODAS reanalysis to represent the surface neutral density and the heat content in the layer from 0 to 300 meters of the Southern Ocean. Reanalysis show an error in neutral density in relation to in situ data ranging between -1 and 2 kg/m^3, with most of the significant errors occurring in the 1990s due to the still low coverage of remote sensing data in the region. The neutral density trends of the reanalysis are distinct, the reason for the differences are their different salinity profiles, considering that they all have very similar temperature trend profiles and density fluxes. The ORAS5 is more different between the reanalysis as it shows a negative salinity and neutral density trend for most of the Southern Ocean. It is believed that the reason for this trend is that their salinity is restricted by a process called nudging. In relation to ocean heat content, all the reanalysis shows an increase with the most intense being GLORYS which shows an increase of 1.38×10^{18} J/yr. The first variability module of the reanalysis is directly linked to ENSO with GLORYS and ORAS5 presenting a higher correlation than GODAS and having a clear Antarctic Dipole. The second mode of variability is only well represented by GLORYS and ORAS5 because it is a mode that is highly linked to oceanic vortices whose GODAS reanalysis does not resolve. GLORYS and ORAS5 are the only ones to show a correlation with SAM. SAM impacts ocean heat content with an Antarctic Dipole as well, but in a way opposite to ENOS. When removing the ENSO signal from the SAM correlation with heat content it is possible to see that it loses the dipole characteristic indicating that the SAM acts more as a regulator of the ENSO impact than by itself in the Southern Ocean. The two ocean models MOM025 and MOM run with the parameters of the CORE-II experiment fail to represent the heat content in the Southern Ocean as well as their modulus of variability because they rule out the impact of ENOS on the heat content.

Keywords: GODAS. GLORYS. ORAS5. ENOS. SAM. Sea Surface Salinity. Density Flux. CORE-II.

LISTA DE SIGLAS E ABREVIATURAS

INTRODUÇÃO

AFA	Água de fundo Antártica
AFS	Sigla em inglês para Frente Antártica
AMSA	Água Modal Subantártica
CCA	Corrente Circumpolar Antártica
CCO	Conteúdo de Calor Oceânico
CDT	Conductive Temperature and Depth
CO2	Dióxido de Carbono
CORE II	Coordinated Ocean-Sea Ice Reference Experiments Phase II
CRM	Circulação de Revolvimento Meridional
ENOS	El Niño Oscilação Sul
GFLD-MOM	Geophysical Fluid Dynamics Laboratory - Modular Ocean Model
GLORYS 2v4	Global Ocean Reanalysis and Simulation 2v4
GODAS	Global Ocean Data Assimilation System
IDW	Sigla em inglês para Água Profunda do Índico
MAS	Modo Anular Sul
MOM	Modular Ocean Model
NADW	Sigla em inglês para Água Profunda do Atlântico Norte
NPIW	Sigla em inglês para Água Intermediária Antártica
PDW	Sigla em inglês para Água Profunda do Pacífico
PF	Sigla em inglês para Frente Polar
SACCF	Sigla em inglês para Frente Sul da CCA
SAF	Sigla em inglês para Frente Subantártica
SB	Sigla em inglês para Fronteira Sul
STF	Sigla em inglês para Frente Subtropical
OA	Oceano Austral
ORAS5	Ocean Reanalysis System 5
WOCE	World Ocean Circulation Experiment

ARTIGO 1

AABW	Antarctic Bottom Water
AAIW	Antarctic Intermediate Water
ACC	Antarctic Circumpolar Current
BMC	Brazil-Malvinas Confluence
CDO	Climate Data Operator
CORA 4	Coriolis Ocean Database ReAnalysis v4
E-P	Evaporation Minus Preciptation
ECMWF	European Center for Medium-Range Weather Forecasts
ERA I	'ECMWF Re-Analysis' 'Interim'
ICTP	International Centre for Theoretical Physics
LCDW	Lawer Circumpolar Deep Water
MAPE	Mean Absolute Percentage Error
MBT	Mechanical Bathythermograph
MOC	Meridional Overturning Circulation
NADW	North Atlantic Deep Water
NCEP	National Centers for Enviromental Prediction
NEMO	Nucleus for European Modelling of the Ocean
OAFlux	Objectivelly Analyzed Air-Sea Fluxes
RMSE	Root Mean Squared Error
SAF	Subantarctic Front
SAMW	Subantarctic Mode Water
SO	Southern Ocean
SSS	Sea Surface Salinity
SST	Sea Surface Temperature
TS	Temperature Salinity
UCDW	Upper Circumpolar Deep Water
XBT	Expendable Bathythermograph

ARTIGO 2

CORA	'Coriolis Ocean Database ReAnalysis
ENSO	El Niño South Oscillation
EOF	Empirical Orthogonal Function
GLORYS-AM	Global Ocean Reanalysis and Simulation Annual Mean

GSW	Gibbs-Sea Water
IAP	Institute of Atmospheric Physics
LIM2	Louvain-La-Neuve sea ice model v2
OHC	Ocean Heat Content
ONI	Oceanic Niño Index
PC-1	First Principal Component
SAM	Southern Annular Mode

SUMÁRIO

1. INTRODUÇÃO

O Oceano Global representa aproximadamente 71% da superfície terrestre e é dividido em cinco oceanos (TALLEY et al., 2011). Ele é um dos reguladores do clima global, responsável por absorver aproximadamente 93% do excesso de energia derivada da atividade humana (RHEIN; RINTOUL; AOKI, 2013). Dentre os cinco oceanos que compõem o Oceano Global, o Oceano Austral (OA) é o foco deste estudo. Ao contrário dos outros oceanos, o OA não tem uma região geográfica delimitada nem continentes ao seu redor que o limitam (Figura 1).

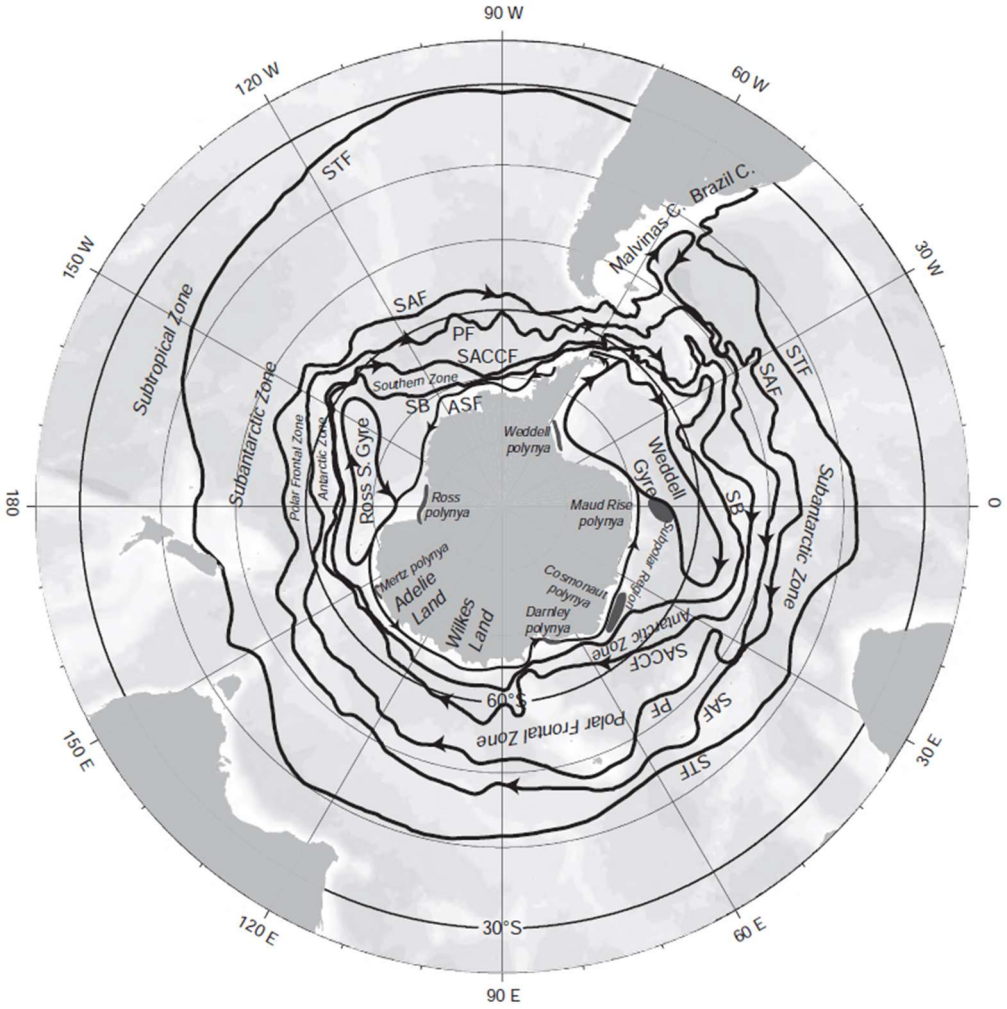

Figura 1 – Geografia do Oceano Austral: principais frentes e zonas oceanográficas. Siglas em inglês: Frente Subtropical (STF), Frente Subantártica (SAF), Frente Polar (PF), Frente Sul da CCA (SACCF), Fronteira Sul (SB) e Frente Antártica (AFS). Fonte: Talley et al. (2011).

A circulação oceânica de larga escala do OA é dominada pela Corrente Circumpolar Antártica (CCA), que vai da superfície até as camadas mais profundas do oceano. Esta corrente, gerada parcialmente pelas interações dos fortes ventos do oeste existentes na região, entre aproximadamente 40 e 60°S, devido à ausência de barreiras naturais, flui continuamente para o leste, circundando toda a Antártica (TALLEY et al., 2011).

Apesar de o "limite" norte do OA não ser bem definido, o Tratado Antártico o limita em 60ºS. Entretanto, se considerar o limite da CCA como sendo o definidor do OA, esse limite se estende até 38ºS em algumas regiões. Recentemente, considera-se o limite do OA como 30ºS, e assim também é considerado neste trabalho, englobando todos os fenômenos que ocorrem ao norte da Frente Subtropical (FST), conforme Talley et al. (2011).

Para Farneti et al. (2015), a CCA é responsável por conectar e promover a troca de energia e de nutrientes entre as três maiores bacias oceanográficas (Figura 2). As águas profundas que se originam em cada um dos oceanos são transportadas para a CCA, são misturadas, ressurgem e modificam-se em águas mais ou menos densas e são transportadas para o norte das bacias oceânicas.

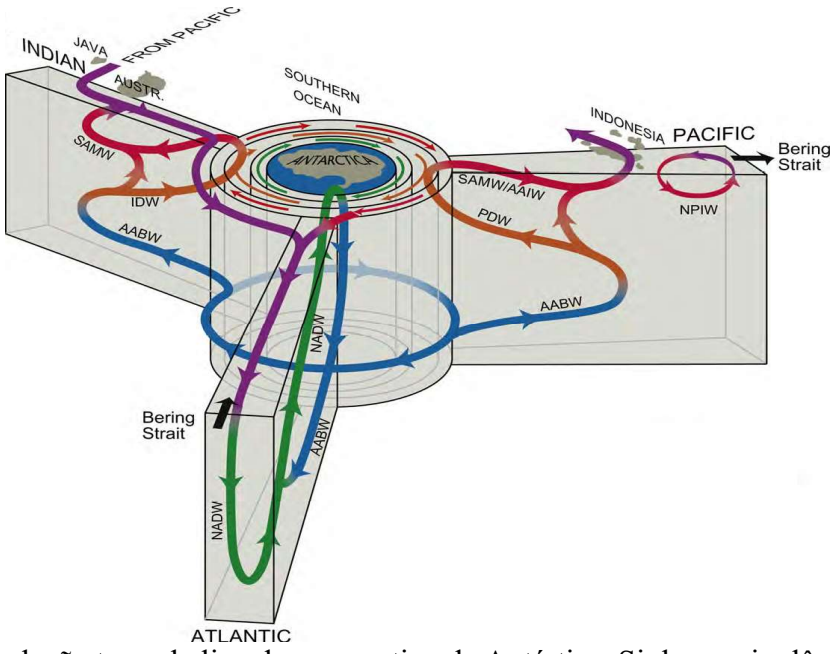

Figura 2 – Circulação termohalina da perspectiva da Antártica. Siglas em inglês: AMSA (Água Modal Subantártica), AAIW (Água Intermediária Antártica), NPIW (Água Intermediária do Pacífico Norte), IDW (Água Profunda do Índico), PDW (Água Profunda do Pacífico), NADW (Água Profunda do Atlântico Norte) e AFA (Água de Fundo Antártica). Fonte: Talley et al. (2011).

Devido à sua posição em altas latitudes e à subsequente formação de gelo marinho, o OA produz suas próprias águas profundas e de fundo prioritariamente ao longo da costa da Antártica, preenchendo assim o fundo oceânico ao norte do continente Antártico (Figura 2). O OA é considerado uma peça-chave para um melhor entendimento do clima terrestre no passado, presente e futuro. Sua importância se deve a diversos fatores como o fato de as interações entre o oceano, a atmosfera e a criosfera, que ocorrem no OA, estabelecerem a magnitude e os padrões da Circulação de Revolvimento Meridional (CRM), de acordo com pesquisas realizadas por Sloyan e Rintoul (2001), Lumpkin e Speer (2007), Marshall e Speer (2012), Abernathey et al. (2016), Pellichero et al. (2018) e Rintoul (2018). De fato, diversos autores consideram que a circulação oceânica e as massas d'água formadas na região são fundamentais para a circulação oceânica global (SLOYAN; RINTOUL, 2001; MARINOV et al., 2006; SARMIENTO et al., 2004; MARSHALL; SPEER, 2012; FARNETI et al., 2015).

Além de sua importância para a circulação oceânica, as massas d'água formadas na região, transportadas para todas as demais bacias oceânicas, são cruciais para um melhor entendimento nas distribuições de calor, dióxido de carbono (CO_2) e oxigênio por todo o oceano global (BANKS; GREGORY, 2006; TALLEY et al., 2011; KHATIWALA et al., 2013; MARSHALL et al., 2015; YAMAMOTO et al., 2015). O OA desempenha também um papel significativo nos estudos de cenários de mudanças climáticas, sendo responsável pela absorção de 40 a 50% do CO_2 antropogênico (SABINE et al., 2004; WATSON; NAVEIRA GARABATO, 2006; FRÖLICHER et al., 2015), além da absorção de mais de 70% do calor relacionado às atividades humanas (DUFOUR et al., 2015; FRÖLICHER et al., 2015).

Apesar de sua reconhecida importância, o OA permanece pobremente amostrado, com poucos modelos satisfatórios da região (SILVANO, 2020), gerando muitas dúvidas sobre os processos que ocorrem nas diversas camadas do OA (FARNETI et al., 2015). Contudo, diversos grupos de pesquisa têm focado na avaliação e aprimoramento dos modelos de reanálises oceânicas, com foco nas representações dos diversos processos que ocorrem na região (JUSTINO et al., 2011; BRACEGIRDLE et al., 2013; SALLÉE et al., 2013; FARNETI et al., 2015; JUSTINO et al., 2015; WANG; DOMMENGET, 2015; SCHNEIDER; REUSCH, 2016; WANG et al., 2018; JUSTINO et al., 2019; ALMEIDA; MAZLOFF; MATA, 2021).

Em uma linha similar, este trabalho busca avaliar as capacidades das reanálises oceânicas GLORYS2v4 – Global Ocean Reanalysis and Simulations 2v4 (FERRY et al., 2010), ORAS5 – Ocean ReAnalysis System 5 (ZUO et al., 2019) e GODAS – Global Ocean Data Assimilation System (BEHRINGER; XUE, 2004) em representarem duas importantes variáveis oceanográficas, entre os anos de 1993 e 2014, período em que as três reanálises apresentaram

resultados simultâneos. Em um primeiro momento (Artigo 1), serão analisadas como as reanálises representam a densidade neutra superficial – γ^n_s (JACKETT; McDOUGALL, 1997), por meio de comparação com dados de CTD (Conductive Temperature and Depth) disponibilizados pelo WOCE (World Ocean Circulation Experiment).

A γ^n_s foi escolhida por ser uma função de temperatura, salinidade, pressão e posição geográfica capaz de determinar mais precisamente superfícies isopicnais e diferentes massas d'água (JACKETT; McDOUGALL, 1997). Logo, uma melhor representação da γ^n_s é de suma importância para representação dos gradientes meridionais de densidade que são diretamente ligados à intensidade da CCA (RINTOUL, 2007); e para representação de diferentes massas d'água formadas na região como a Água Antártica de Fundo que é definida por diversos autores por meio de sua densidade neutra (GORDON, 2001; RINTOUL, 2007; MARSHALL; SPEER, 2012; AZANEU et al., 2013).

A segunda parte deste trabalho (Artigo 2) tratará não somente da maneira como as reanálises representam o Conteúdo de Calor Oceânico (CCO), mas também de dois modelos oceanográficos: o Geophysical Fluid Dynamics Laboratory – Modular Ocean Model (GFLD-MOM) que participou do Coordinated Ocean-Sea Ice Reference Experiments Phase II – CORE-II (DANABASOGLU et al., 2014) e o GFLD-MOM025, derivado do GFLD-MOM com uma resolução maior. A CCO foi escolhida por representar o aquecimento do OA, uma vez que estudos recentes mostram que existem muitas discrepâncias da CCO em diversos níveis do OA, podendo acarretar interpretações pouco realistas de movimentações oceânicas (WANG et al., 2018). O estudo e a melhor compreensão da CCO e dos processos relacionados à sua variabilidade são de fundamental importância para uma melhoria das parametrizações oceânicas e dos modelos oceânicos e acoplados (GRIFFIES et al., 2005; SCHUCKMANN et al., 2016).

Referências

ABERNATHEY, R. P.; CEROVECKI, I.; HOLLAND, P.R.; NEWSOM, E.; MAZLOFF, M.; TALLEY, L.D. Water-mass transformation by sea ice in the upper branch of the Southern Ocean overturning. **Nat. Geosci.**, v. 9, p. 596-601, 2016.

ALMEIDA, L.; MAZLOFF, M. R.; MATA, M. M. The impact of Southern Ocean Ekman pumping, heat and freshwater flux variability on intermediate and mode water export in CMIP models: present and future scenarios. **Journal of Geophysical Research: Oceans**, v. 126, e2021JC017173, 2021. doi:10.1029/2021JC017173.

AZANEU, M. V. C.; PEREIRA, R. K. D.; MATA, M. M.; GARCIA, C. A. E. Trends in the deep Southern Ocean (1958-2010): implications for Antarctic bottom water properties and volume export. **J. Geophys. Res.**, v. 118, p. 4213-4227, 2013.

BANKS, H. T.; GREGORY, J. M. Mechanisms of ocean heat uptake in a coupled climate model and the implications for tracer-based predictions of ocean heat uptake. **Geophys. Res. Lett.**, v. 33, L07608, 2006. doi:10.1029/2005GL025352.

BEHRINGER, D.; XUE, Y. Evaluation of the global ocean data assimilation system at NCEP: the Pacific Ocean. In: SYMPOSIUM ON INTEGRATED OBSERVING AND ASSIMILATION SYSTEMS FOR ATMOSPHERE, OCEAN, AND LAND SURFACE, 8, 2004, Seattle. **Proceedings…** Seattle: American Meteorological Society, 2004.

BRACEGIRDLE, T. J.; SHUCKBURGH, E.; SALLEE, J.-B.; WANG, Z.; MEIJERS, A. J. S.; BRUNEAU, N.; … WILCOX, L. J. Assessment of surface winds over the Atlantic, Indian, and Pacific Ocean sectors of the Southern Ocean in CMIP5 models: historical bias, forcing response, and state dependence. **J. Geophys. Res. Atmos.**, v. 118, p. 547-562, 2013. doi:10.1002/jgrd.50153.

DANABASOGLU, G.; YEAGER, S. G.; BAILEY, D.; BEHRENS, E.; BENTSEN, M.; BI, D.; … WANG, Q. North Atlantic simulations in Coordinated Ocean-ice Reference Experiments phase II (CORE-II). **Part I Mean States: Ocean Modelling**, v. 73, p. 76-107, 2014.

DUFOUR, C. O.; GRIFFIES, S. M.; SOUZA, G. F.; FRENGER, I.; MORRISON, A. K.; PALTER, J. B.; … SLATER, R. D. Role of mesoscale eddies in cross-frontal transport of heat and biogeochemical tracers in the Southern Ocean. **Journal of Physical Oceanography**, v. 45, n. 12, p. 3057-3081, 2015. doi:10.1175/JPO-D-14-0240.1.

FARNETI, R.; DOWNES, S. M.; GRIFFIES, S. M.; MARSLAND, S. J.; BEHRENS, E.; BENTSEN, M.; … YEAGER, S. G. An assessment of Antarctic Circumpolar Current and Southern Ocean meridional overturning circulation during 1958-2007 in a suite of interannual CORE-II simulations. **Ocean Modelling**, v. 93, p. 84-120, 2015. doi:10.1016/j.ocemod.2015.07.009.

FERRY, N.; PARENT, L.; GARRIC, G.; BARNIER, B.; JOURDAIN, N. Mercator global Eddy permitting ocean reanalysis GLORYS1V1: description and results. **Mercator-Ocean Q Newslett.**, v. 36, p. 15-27, 2010.

FRÖLICHER, T. L.; SARMIENTO, J. L.; PAYNTER, D. J., DUNNE, J. P., KRASTING, J. P., & WINTON, M. Dominance of the Southern Ocean in anthropogenic carbon and heat uptake in CMIP5 models. **Journal of Climate**, v. 28, n. 2, p. 862-886, 2015. doi:10.1175/jcli-d-14-00117.1.

GORDON, A. L. Bottom water formation. **Encyclopedia of Ocean Sciences**, p. 415-421, 2001. doi:10.1016/b978-012374473-9.00006-0.

GRIFFIES, S.; GNANADESIKAN, A.; DIXON, K.; DUNNE, J.; GERDES, R.; HARRISON, M.; … ZHANG, R. Formulation of an ocean model for global climate simulations. **Ocean Science**, v. 1, 2005. doi:10.5194/osd-2-165-2005.

JACKETT, D. R.; McDOUGALL, T. J. A neutral density variable for the world's ocean. **Journal of Physical Oceanography**, v. 27, n. 2, p. 237-263, 1997. doi:10.1175/1520-0485(1997)0272.0.CO;2.

JUSTINO, F.; SETZER, A.; BRACEGIRDLE, T. J.; MEDES, D.; GRIMM, A.; DECHICHE, G.; SCHAEFER, C.E.G.R. Harmonic analysis of climatological temperature over Antarctica: present day and greenhouse warming perspectives. **Int. J. Climatol.**, v. 31, p. 514-530, 2011. doi:10.1002/joc.2090.

JUSTINO, F.; SILVA, A. S.; PEREIRA, M. P.; STORDAL, F.; LINDEMANN, D.; KUCHARSKI, F. The large-scale climate in response to the retreat of the west Antarctic ice sheet. **Journal of Climate**, v. 28, n. 2, p. 637-650, 2015. doi:10.1175/jcli-d-14-00284.1.

JUSTINO, F.; WILSON, A. B.; BROMWICH, D. H.; AVILA, A.; BAI, L.-S.; WANG, S.-H. Northern Hemisphere extratropical turbulent heat fluxes in ASRv2 and global reanalysis. **J. Climate**, v. 32, p. 2145-2166, 2019. doi:10.1175/JCLI-D-18-0535.1.

KHATIWALA, S.; TANHUA, T.; MIKALOFF FLETCHER, S.; GERBER, M.; DONEY, S. C.; GRAVEN, H. D.; … SABINE, C. L. Global Ocean storage of anthropogenic carbon, **Biogeosciences**, v. 10, p. 2169-2191, 2013. doi:10.5194/bg-10-2169-2013.

LUMPKIN, R.; SPEER, K. Global Ocean meridional overturning. **J. Phys. Oceanogr.**, v. 37, p. 2550-2562, 2007.

MARINOV, I.; GNANADESIKAN, A.; TOGGWEILER, J. R.; SARMIENTO, J. L. The Southern Ocean biogeochemical divide. **Nature**, v. 441, p. 964-967, 2006.

MARSHALL, J.; SPEER, K. Closure of the meridional overturning circulation through Southern Ocean upwelling. **Nature Geosci.**, v. 5, p. 171-180, 2012. doi:10.1038/ngeo1391.

MARSHALL, J.; SCOTT, J. R.; ARMOUR, K. C.; CAMPIN, J.-M.; KELLEY, M.; ROMANOU, A. The ocean's role in the transient response of climate to abrupt greenhouse gas forcing. **Clim. Dyn.**, v. 44, n. 7-8, p. 2287-2299, 2015. doi:10.1007/s00382-014-2308-0.

PELLICHERO, V.; SALLÉE, J.-B.; CHAPMAN, C. C.; DOWNES, S. M. The Southern Ocean meridional overturning in the sea-ice sector is driven by freshwater fluxes. **Nat. Commun.**, v. 9, p. 1789, 2018. doi:10.1038/s41467-018-04101-2.

RHEIN, M.; RINTOUL, S. R.; AOKI, S. Observations: ocean. In: CLIMATE Change 2013. **The physical science basis**. Contribution of working group I to the fifth assessment report of the intergovernmental panel on climate change. Cambridge, NY: Cambridge University Press, 2013.

RINTOUL, S. R. Rapid freshening of Antarctic Bottom Water formed in the Indian and Pacific oceans. **Geophys. Res. Lett.**, v. 34, L06606, 2007. doi:10.1029/2006GL028550l.

RINTOUL, S. R. The global influence of localized dynamics in the Southern Ocean. **Nature**, v. 558, p. 209-218, 2018. doi:10.1038/s41586-018-0182-3.

SABINE, C. L.; FEELY, R. A.; GRUBER, N.; KEY, R. M.; LEE, K.; BULLISTER, J. L.; … RIOS, A. F. The oceanic sink for anthropogenic CO2. **Science**, v. 305, n. 5682, p. 367-371, 2004. doi:10.1126/science.1097403.

SALLÉE, J.-B.; SHUCKBURGH, E.; BRUNEAU, N.; MEIJERS, A. J. S.; BRACEGIRDLE, T. J.; WANG, Z.; ROY, T. Assessment of Southern Ocean water mass circulation and characteristics in CMIP5 models: historical bias and forcing response. **J. Geophys. Res. Oceans**, v. 118, p. 1830-1844, 2013. doi:10.1002/jgrc.20135.

SARMIENTO, J. L.; GRUBER, N.; BRZEZINSKI, M. A.; DUNNE, J. P. High-latitude controls of thermocline nutrients and low latitude biological productivity. **Nature**, v. 427, p. 56-60, 2004.

SCHNEIDER, D. P.; REUSCH, D. B. Antarctic and Southern Ocean Surface Temperatures in CMIP5 Models in the Context of the Surface Energy Budget. **Journal of Climate**, v. 29, n. 5, p. 1689-1716, 2016.

SCHUCKMANN, K.; PALMER, M.; TRENBERTH, K. E.; CAZENAVE, A.; CHAMBERS, D.; CHAMPOLLION, N.; … WILD, M. An imperative to monitor Earth's energy imbalance. **Nature Clim. Change**, v. 6, p. 138-144, 2016. doi:10.1038/nclimate2876.

SILVANO, A. Changes in the Southern Ocean. **Nat. Geosci.**, v. 13, p. 4-5, 2020. doi: 10.1038/s41561-019-0516-2.

SLOYAN, B. M.; RINTOUL, S. R. The Southern Ocean limb of the global deep overturning circulation. **J. Phys. Oceanogr.**, v. 31, p. 143-173, 2001.

TALLEY, L. D.; PICKARD, G. L.; EMERY, W. J.; SWIFT, J. H. **Descriptive physical oceanography**: an introduction. 6. ed. Boston: Elsevier, 2011. 560 p.

WANG, G.; DOMMENGET, D. The leading modes of decadal SST variability in the Southern Ocean in CMIP5 simulations. **Climate Dynamics**, v. 47, n. 5-6, 1775-1792, 2015. doi:10.1007/s00382-015-2932-3.

WANG, G.; CHENG, L.; ABRAHAM, J.; CHONGYIN, L. Consensuses and discrepancies of basin-scale ocean heat content changes in different ocean analyses. **Climate Dynamics**, v. 50, p. 2471-2487, 2018. doi:10.1007/s00382-017-3751-5.

WATSON, A. J.; NAVEIRA GARABATO, A. C. The role of Southern Ocean mixing and upwelling in glacial-interglacial atmospheric CO2 change. **Tellus B**, v. 58, p. 73-87, 2006. doi:10.1111/j.1600-0889.2005.00167.x.

YAMAMOTO, A.; ABE-OUCHI, A.; SHIGEMITSU, M.; OKA, A.; TAKAHASHI, K.; OHGAITO, R.; YAMANAKA, Y. Global deep ocean oxygenation by enhanced ventilation in the Southern Ocean under long-term global warming. **Global Biogeochem. Cycles**, v. 29, p. 1801-1815, 2015. doi:10.1002/2015GB005181.

ZUO, H.; BALMASEDA, M. A.; TIETSCHE, S.; MOGENSEN, K.; MAYER, M. The ECMWF operational ensemble reanalysis–analysis system for ocean and sea ice: a description of the system and assessment. **Ocean Sci.**, v. 15, p. 779-808, 2019. doi:10.5194/os-15-779-2019.

ARTIGO 1

Representation of Southern Ocean surface neutral density by three global oceanic reanalysis and WOCE dataset

Rafael Afonso do Nascimento Reis [1]*, Flávio Barbosa Justino [2], Luís Felipe Ferreira de Mendonça [3], Riccardo Farneti [4], Marcos Henrique Maruch Tonelli [5],Jeferson Prietsch Machado [6] & Douglas da Silva Lindemann [7]

[1] rafael_cgb@hotmail.com https://orcid.org/0000-0003-4115-2265 Universidade Federal de Viçosa - Departamento de Engenharia Agrícola – Sala 107 ZIPCODE: 36570-900 – Viçosa – Minas Gerais - Brasil
[2] fjustino@ufv.br https://orcid.org/0000-0003-0929-1388 Universidade Federal de Viçosa - Departamento de Engenharia Agrícola – Sala 107 ZIPCODE: 36570-900 – Viçosa – Minas Gerais - Brasil
[3] luis.mendonca@ufba.br https://orcid.org/0000-0001-7836-200X Universidade Federal da Bahia - Instituto de Geociências - Departamento de Oceanografia Rua Barão de Jeremoabo, s/n, Campus Universitário de Ondina ZIPCODE: 40.170-020, Salvador – Bahia - Brasil,
[4] rfarneti@ictp.it https://orcid.org/0000-0001-7781-6436, ICTP, Earth System Physics Section, Strada Costiera, 11 ZIPCODE: 34151, Trieste - ITALY
[5] marcos.tonelli@gmail.com https://orcid.org/0000-0002-0984-6358 Instituto Oceanográfico da Universidade de São Paulo – São Paulo – São Paulo - Brasil
[6] jefpmac@gmail.com https://orcid.org/0000-0003-2685-3944 Universidade Federal do Rio Grande - Instituto de Oceanografia – Núcleo de Oceanografia Geológica Avenida Itália, km 8, ZIPCODE: 96203-900, Rio Grande – Rio Grande do Sul - Brasil
[7] douglas.lindemann@ufpel.edu.br https://orcid.org/0000-0002-7503-143X, Universidade Federal de Pelotas Departamento de Meteorologia CEP 96160-000, Pelotas - Rio Grande do Sul - Brasil.

Abstract: This article analyzes the capabilities of three oceanic reanalysis, GLORYS, ORAS5 and GODAS, in representing the surface neutral density across the Southern Ocean, based on a comparison with WOCE data. Difference among reanalysis and the WOCE are between -1 and 2 kg/m³, with most significant errors occurring in the 1990s. The maximum error ranged from -3,8 to 7,6% in relation to the WOCE mean value of the surface neutral density. The RMSE values are between 0,28 and 1,78, and MAPE between 0,6 and 2,6%. A 99% correlation between all the reanalysis and WOCE data indicates that they are very suitable to be used in Southern Ocean. The neutral density trend presents the biggest difference between the reanalysis, ORAS5 presents negative trend for almost all the Southern Ocean, GODAS have the biggest trends and is unique to indicates a negative trend in the Weddell Sea and the Pacific Ocean, between 45 and 60ºS. These differences may arise due to the SSS trend, each model uses a different input for salinity data. While the GODAS uses the synthetic salinity which can seriously underestimate the variability of salinity, the ORAS5 salinity is constrained by climatology nudging, and this may limit is interpretation of the SSS trend. Overall, all reanalysis has a satisfactory representation of the surface neutral density. Thus, reanalysis can be an important tool for studying the Southern Ocean in particular surface regions of water mass formation that can be characterized by the neutral density.

Academy Section: Oceanography.

Keywords: Density Fluxes. GODAS. GLORYS. ORAS5. Sea Surface Salinity.

1. Introduction

Over the years, several studies have been carried out across the Southern Ocean (SO; south of 30ºS) demonstrating that processes occurring in the SO are controlled by a complex, and not full elucidated interactions, between the ocean, atmosphere, and land/sea ice conditions (Rintoul, 2018). It is worth mentioning that the SO has a significant role in the global climate. For example, the SO has significant importance in the carbon dioxide (CO_2) variability between the ocean and atmosphere, because it absorbs by about 40-50% anthropogenic CO_2 (Sabine *et al*., 2004; Watson & Naveira Garabato, 2006; Frölicher *et al*., 2015, among others). Moreover, the SO uptakes more than 70% of the heat related to anthropogenic activities (Dufour *et al*., 2015; Frölicher *et al*., 2015).

Due to the lack of physical barriers the SO allows for development of the Antarctic Circumpolar Current (ACC), that acts as a link between the others oceanic basins transporting water from one basin to another (Farneti *et al*., 2015). The circulation and water mass transformation in the region are very relevant for the global oceanic circulation (Sloyan & Rintoul, 2001; Marinov *et al*., 2006; Sarmiento *et al*., 2011; Marshall & Speer, 2012; Farneti *et al*., 2015, among others). The ocean-atmosphere-cryosphere interaction in the SO through the surface buoyancy and wind-stress sets the magnitude and pattern of the Meridional Overturning Circulation – MOC (Sloyan & Rintoul, 2001; Lumpkin & Speer, 2007; Marshall & Speer, 2012; Abernathey *et al*., 2016; Pellichero *et al*., 2018; Rintoul, 2018, amoung others).

Part of the MOC in the SO is the ascending branch of the deep water generated in the North Atlantic, known as North Atlantic Deep Water (NADW), that flows southward and is transformed in the Upper Circumpolar Deep Water (UCDW) and Lower Circumpolar Deep Water (LCDW) (Talley *et al*., 2011). The UCDW ascends to the surface and through air-sea buoyancy fluxes, is converted into the Antarctic Intermediate Water (AAIW) and Subantarctic Mode Water (SAMW) that flows northward, submerging in the subtropical front and occupying the upper layers of the oceanic gyres ventilating these regions (Sloyan & Rintoul, 2001; Hartin *et al*., 2011; Farneti *et al*., 2015). The LCDW emerges near the Antarctic coast and through air-sea-ice interactions is integrated into the Antarctic Bottom Water (Gordon, 2001; Marshall & Speer, 2012). The ascension of water in the MOC is responsible for increasing nutrients from the intermediate and deep ocean to the ocean surface worldwide, which according to model simulations is responsible for three-quarters of primary production north of 300S (Sarmiento *et al*., 2004; Marinov *et al*., 2006).

These water masses formation and transport in the SO as well as how the ocean-atmosphere-cryosphere interaction modulates these processes, are key points for the

understanding of distribution of heat, CO_2, and oxygen throughout the global ocean (Banks & Gregory, 2006; Talley *et al*., 2011; Khatiwala *et al*., 2013; Marshall *et al*., 2015; Yamamoto *et al*., 2015). However, besides the SO importance the overall knowledge of the region still has many challenges because it is poorly sampled, and accurate modeling results are scarce (Silvano, 2020). Many research groups aimed to overcome these difficulties focusing on how the oceanic models and reanalysis represent the SO (Justino *et al*., 2011; Bracegirdle *et al*., 2013; Sallée *et al*., 2013; Farneti *et al*., 2015; Schneider & Reusch, 2016; Almeida; Mazloff; Mata, 2021, among others). However due to the lack of *in situ* observations several questions remain, in particular in regards the influence of atmosphere on leading changes in surface density which subsequently modifies the characteristics and magnitude of water mass formation.

In this sense, the present work aims to analyze the capabilities of GLORYS2v4 – Global Ocean Reanalysis and Simulations 2v4 – here after GLORYS (Ferry *et al*., 2010,), ORAS5 – Ocean ReAnalysis System 5 (Zuo *et al*., 2019) and GODAS – Global Ocean Data Assimilation System (Behringer & Xue, 2004) reanalysis in representing averaged and trends of surface neutral density – γ^n_s (Jackett & McDougall, 1997), through comparisons with CTD (Conductive Temperature and Depth) data from the WOCE (World Ocean Circulation Experiment) data set across the SO. The γ^n_s was chosen because the meridional density gradient is linked to the strength of the ACC (Rintoul, 2018), and is an oceanographic variable capable to separate different neutral density surfaces which allows for a better identification of water masses. Thus, if the models have a good representation of these variable, they can be used for studying water mass transformation related to buoyancy fluxes, as well as may shed light on the impact of changes in the meridional density gradient in the SO superficial circulation.

2. Methodology

2.1. Oceanographic reanalysis

This work applies three global oceanic reanalysis based on monthly averaged, namely: the Mercator Ocean – Global Ocean Physics Reanalysis 2 version 4 – GLORYS2V4 (https://www.mercator-ocean.fr/en/ocean-science/glorys/), the European Centre for Medium-Range Weather Forecasts – ECWMF – Ocean ReAnalysis System 5 – ORAS5 (https://www.ecmwf.int/en/forecasts/dataset/ocean-reanalysis-system-5) and the NCEP – National Centers for Environmental Prediction – Global Ocean Data Assimilation System – GODAS (https://www.cpc.ncep.noaa.gov/products/GODAS/). A brief description of the data is provided below in the Table 1.

Table 1: Brief description of the reanalysis

	Model	Horizontal Resolution	Vertical levels	Reference
GLORYS2v4	NEMO 3.1 + LIM2	1/4º by 1/4º	75	**Garric *et al.* (2017)**
ORAS5	NEMO 3.4.1 +LIM2	25 km in the tropics, and increases to 9 km in the Arctic	75	**Zuo *et al.* (2019)**
GODAS	GFDL MOM.v3	1º by 1º enhanced to 1/3º in the N-S direction within 10º of the equator	40	**Behringer & Xue (2004)**

In situ database is obtained from the World Ocean Database – WOCE (Boyer *et al.*, 2018) within the period spanning 1993 and 2014 because this interval is assimilated by the three reanalysis. A CTD device detects the conductivity and temperature in the water column (Millard & Yang, 1993). The CTD WOCE data was chosen because the focus is on investigating the neutral density and a database that has both potential temperature and salinity should be taken into.

2.2. Atmospheric data

Evaporation minus precipitation (E-P) data is taken from the European Center for Medium-Range Weather Forecasts (ECMWF) 'Interim' reanalysis – ERAI (Uppala *et al.*, 2008; Dee *et al.*, 2011). This database was chosen because Nicolas & Bromwich (2011) showed that among 6 atmospheric reanalysis, ERAI shows a better representation of E-P patterns in the Southern Ocean and this is also the atmospheric forcing for all ocean reanalysis. Heat flux data in the present study at ocean-atmosphere interface is collected from the Objectively Analyzed Air-sea Fluxes – OAFlux (Yu; Jin; Weller, 2008). For more information see https://oaflux.whoi.edu/overview/.

Both atmospheric data (ERAI and OAFlux) are in a horizontal resolution of 1º by 1º so we utilize the Climate Data Operator (CDO) software to remap the oceanic reanalysis just for the calculus of the Density Flux (see chapter 2.3).

2.3. Neutral density

Among all physical variables of sea water, neutral density was chosen because it is a function of salinity, temperature, pressure, latitude, and longitude (Eq. 1) that determine the isopycnal surfaces in the water column, and across different bodies of water (Jackett & McDougall, 1997).

$$\nabla\gamma^n = b\rho(\beta\nabla S - \alpha\nabla\,\theta) \qquad \text{Eq. (1)}$$

Where, b is an integrating factor, ρ is the density of seawater, β is the coefficient of saline contraction, α is the coefficient of thermal expansion, S is the salinity in psu and θ is the potential temperature.

2.4 Density fluxes

Surface density variations are influenced by heat and freshwater fluxes exchange between the atmosphere and the ocean. In what follows, we use the density fluxes calculation as proposed by Schmitt, Bodgen & Dorman (1989) – equation 2, and use by many other studies such as Justino *et al.* (2015).

$$F\rho = \alpha F_t + \beta F_s = \alpha(Q/C_p) + \beta\rho[(E-P)S/1-S] \qquad \text{Eq. (2)}$$

Where, α is the thermal expansion coefficient, β is the haline contraction coefficient, F_t and F_s are the heat and salt fluxes. Q, C_p and ρ are the net heat flux, specific heat and density of sea water, E and P are the evaporation and precipitation respectively.

3. Results

3.1 Surface neutral density (reanalysis x in situ observations)

As previously mentioned, the SO lacks data both temporally and spatially. Figure 1 shows an irregular distribution of data from months to years. For example, in Sector 1, which is located between 0º and 60ºE (see Fig. 2), there is a gap of 2 years without observations (from 2002 to the beginning of 2004, Fig. 1a). A sector where this absence of information is most evident is Sector 4 (located between 120ºW and 180º, Fig. 1d), presenting the least amount of data collected (1522, Table 1).

However, sparse temporal sampling is not the only challenge, as shown in Figure 2 (a, b). It is observed in the Pacific Ocean (Sector 5 and 6) that despite being the two sectors with the largest number of data, most of them are located in a few transects, the largest across 37ºS, and on the west coast of the American continent. This data paucity limits the capacity to interpolate the density fields and analyze the spatial differences. Therefore, a point analysis is performed by extracting the data from reanalysis at the center grid box, along the WOCE data to verify the reanalysis performance.

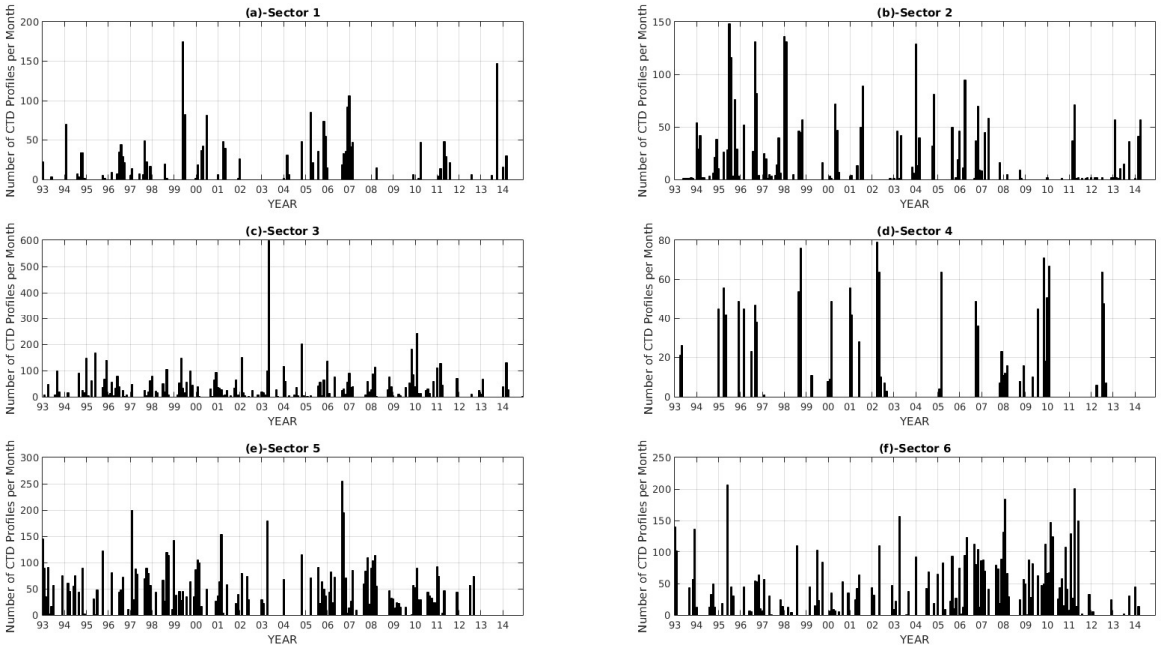

Figure 1: Number of points sampled in each sector each month from January 1993 to December 2014.

Differences in the γ^n_s between the reanalysis and WOCE show a variation between -1 and 2 kg/m³, which represents approximately -3,8 to 7,6% in relation to the mean value. It is worth mentioning that during the 1990s, in particular between the years 1995 and 1999, in sector 6, differences show values up to 4 kg/m³. These peaks are not shown in Figure 2 (a-h), in order to have a clear visualization of dataset, the scale values were restricted to -1 and 2 kg/m³.

Table 2: Average, standard deviation, mean error, RMSE MAPE and r of the surface neutral density for each sector and for the entire Southern Ocean, as well as the number of points in each sector. In contrast the smaller value of RMSE and MAPE

		Sector 1	Sector 2	Sector 3	Sector 4	Sector 5	Sector 6	All Southern Ocean
Mean and Standard Deviation	**WOCE**	26,14±1,19	26,07±0,97	26,38±1,1	26,74±1,05	26,18±0,99	25,84±2,07	**26,17±1,36**
	GLORYS	26,29±1,15	26,06±0,95	26,29±1,02	26,57±0,97	26,19±0,85	25,82±1,99	**26.,15±1,28**
	GODAS	26,37±1,22	26,3±1,02	26,22±1,03	26,69±0,96	26,35±0,85	26.64±1,01	**26,4±1,01**
	ORAS5	26,36±1,13	26,27±0,85	26,23±0,87	26,56±0,96	26,34±0,80	25,86±2,06	**26,23±1,28**
RMSE	**GLORYS**	0,3040	0,3248	0,3417	0,3295	0,6374	1,1320	**0,6717**
	GODAS	0,3285	0,3963	0,3627	0,3170	0,4071	1,1782	**0,6477**
	ORAS5	0,28	0,4811	0,6033	0,4289	0,5863	1,1496	**0,6694**
MAPE (%)	**GLORYS**	0,74	0,74	0,76	0,82	1,67	2,5	**1,4**
	GODAS	0,87	1,15	1,03	0,84	1,1	2,26	**1,31**
	ORAS5	0,63	1,25	1,83	0,98	1,6	2,6	**1,42**
r	**GLORYS**	0,9999	0,9998	0,9998	0,9998	0,9994	0,9981	**0,9993**
	GODAS	0,9998	0,9998	0,9998	0,9999	0,9998	0,9980	**0,9994**
	ORAS5	0,9999	0,9997	0,9995	0,9997	0,9995	0,9981	**0,9993**
Number of Points		2159	3018	6589	1522	7056	6485	**26829**

The reanalysis provides a satisfactory representation of the γ^n_s values, with the RMSE lower less than 0.6 kg/m³ for all sectors (Table 1). The exception was observed in sector 6, where values of RMSE are more than 1.1 kg/m³. Higher MAPE values, greater than 2%, are also found in sector 6, but the correlation between reanalysis and WOCE data is higher than 99% with 95% significance across all sectors. The sector 6 shows the highest RMSE and MAPE values, reaching values 2 to 3 times higher than in the other sectors This is evident in Figure 2 a, c, which shows the spatial distribution of the bias between the reanalysis and WOCE data. The greatest bias is found over the coastal regions of Antarctica, where reanalysis underestimate density values, and across the east coast of South America, where reanalysis tends to overestimate density values, Souza *et al.* (2021) has shown a considerable bias in temperature and salinity in the New Zealand coast showing a limitation of this reanalysis in coastal regions. These sectors also show a greater error in the 90's (Fig. 2h-i) according to Nicolas & Bromwich (2011), this is related to the fact that, although the era of satellite observations has already begun, it was only in the late 1990s and early 2000s that the high latitude regions of the southern hemisphere were better sampled.

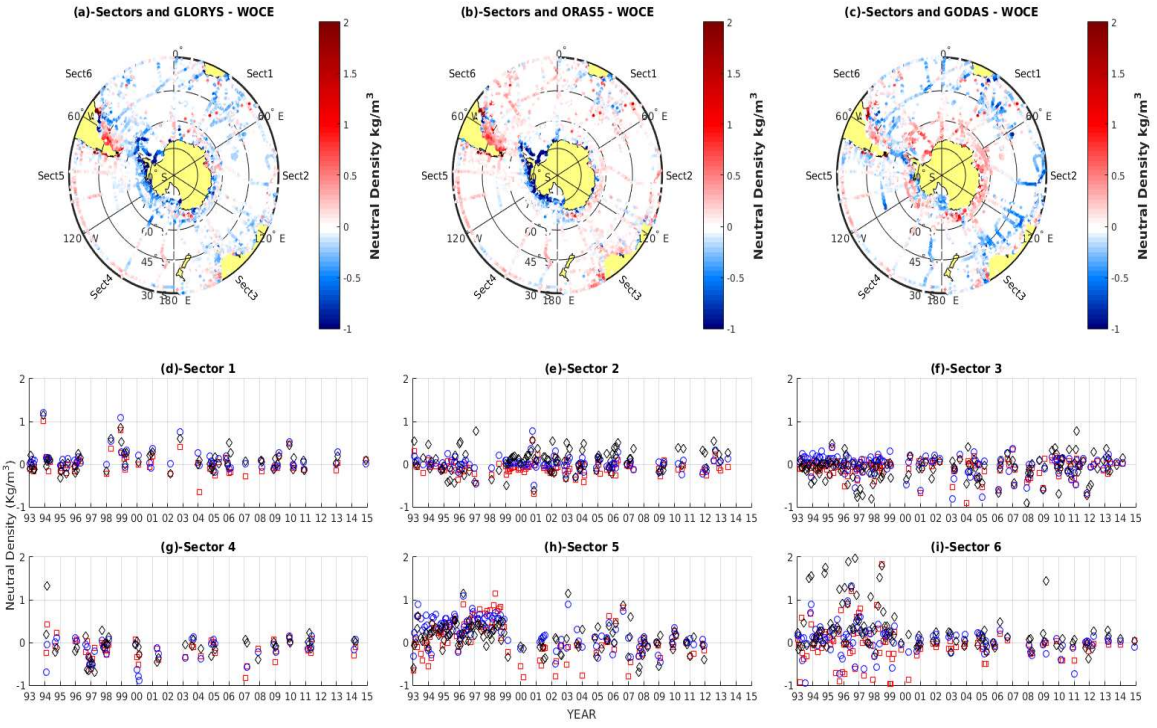

Figure 2: Polar map showing the sectors and the WOCE data collection points along with the differences for neutral density (kg/m³) between GLORYS-WOCE (a), ORAS5-WOCE (b) and GODAS-WOCE (c). GLORYS, ORAS5 and GODAS Bias for every sector (1-6 d-i respectively). Red square, blue circle and black diamond representing the GLORYS ORAS5 and GODAS bias respectively.

GLORYS and ORAS5, in sectors 5 and 6, deliver larger differences than GODAS, perhaps related to the fact that the GODAS exhibits a lower resolution in comparison the others reanalysis. This is more relevant over coastal regions. In several points of the coastal region, GODAS is not able to provide values avoiding comparison between datasets. Except for sector 5 and 6, GLORYS and ORAS5 have bias values close to 0, with GLORYS (ORAS5) mostly presenting a negative (positive) bias. The GODAS reanalysis, on the other hand, shows a predominance of negative bias at north 50°S and positive bias at south 60°S.

3.2. Neutral density spatial patterns

Mean γ^n_s patterns generated by the reanalysis (Fig. 3) are similar and consistent with in situ results, with density varying from 24 kg/m³ to 26 kg/m³ in the northern portion of the Sub-Antarctic Front – SAF (Orsi; Whitworth; Nowlin Jr, 1995), located at approximately 45ºS. Increased density ranges from 26.5 kg/m³ to 28 kg/m³ are noticed in the vicinity of the Antarctic continent. These results are in agreement with Orsi, Whitworth & Nowlin Jr (1995), Peixoto & Oort (1992) and Talley *et al.* (2011).

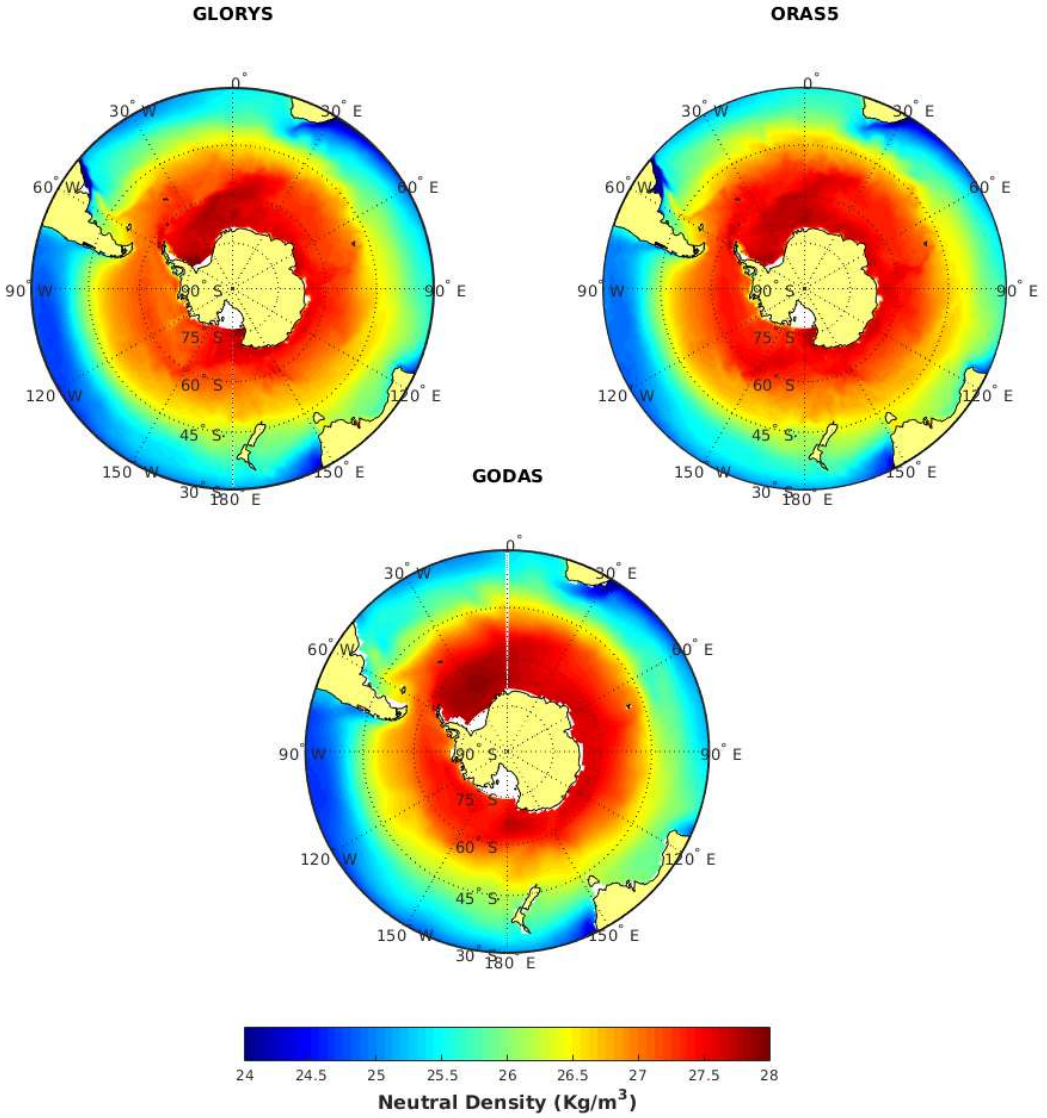

Figure 3: Mean surface neutral density for the period 1993-2014 for GLORYS (a) ORAS5 (b) and GODAS (c).

However, despite similar mean γ^n_s, the same is not true for γ^n_s trend (Fig. 4). GLORYS and ORAS5 presents, a positive trend in the Weddell Sea, which is considered a key area from an oceanographic point of view due to its potential to form water masses such as Antarctic Bottom Water – AABW (Jacobs; Amos; Bruchhausen, 1970; Foster & Carmack, 1976; Rintoul, 1998; Foldvik *et al.,* 2004; Gordon *et al.*, 2009; Williams *et al.*, 2010). These datasets show a positive density trend with values between 0.01 and 0.02 kg/m³ per year, GODAS shows a negative trend between -0.02 and -0.03 kg/m³ per year in the Weddell Sea. The GLORYS and ORAS5 also point to a positive trend near the coast of the Antarctic continent, between the Ross and the Bellinghausen Seas (180° and 60°W), with a significant positive trend, reaching 0.035

kg/m³ per year, at 120°W, in both reanalysis. While GODAS shows a negative trend in this region except for the Bellinghausen Sea near the Antarctic Peninsula.

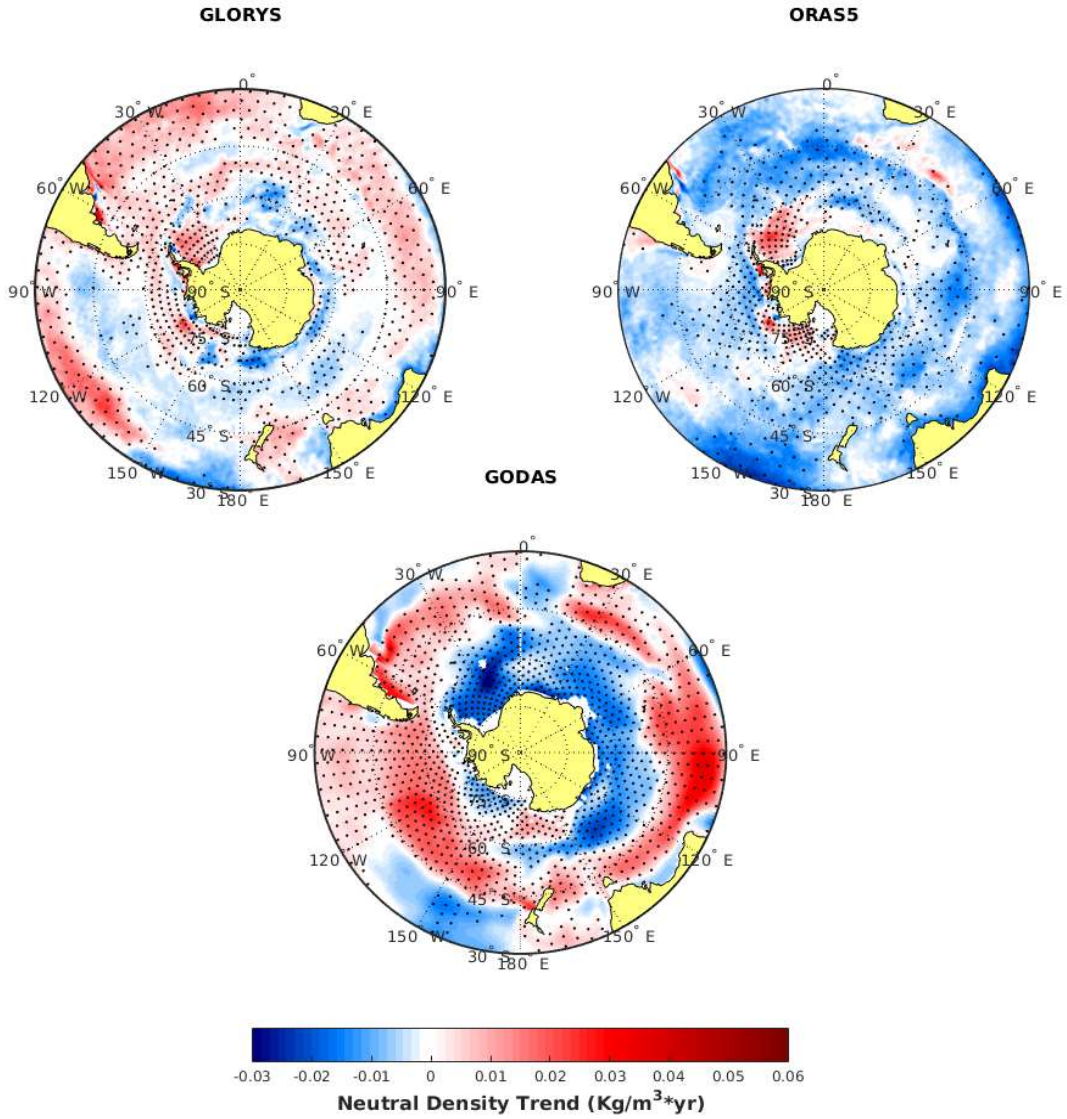

Figure 4: Neutral surface density trend for GLORYS (a), ORAS5 (b) and GODAS (c). Dotted areas show regions with 95% significant trends.

From 90°E clockwise to 90°W, in the range between 45°S and 60°S, GLORYS and ORAS5 show a negative trend, with ORAS5 having more significant regions and values reaching -0.025 kg/m³ per year. GLORYS shows few peaks with by up to -0.015 kg/m³ per year. ORAS5 mostly presents negative trend values for the entire SO, except for the western Antarctic continent, the Brazil-Malvins Confluence (BMC) region, and a small portion in the Indic Ocean close to the African continent.

GODAS shows more intense trend values than those of GLORYS and ORAS5, with a main positive peak near 90°E 30°S, while GLORYS despite agreeing with this positive trend

shows lower values. The GODAS also considers almost all the Pacific portion of the OS under a positive trend, this differs to GLORYS and ORAS5 which demonstrate a negative trend with few significant points between 60-45°S. Between 45-30°S, the GLORYS presents a positive trend as well as GODAS, ORAS5 presents a negative trend but without statistical significance for the same region. In order to explain these differences between the reanalysis γ^n_s trends, trends of density fluxes at the ocean-atmosphere interface, sea surface temperature (SST) and sea surface salinity (SSS) are analyzed.

3.3. Density fluxes trends

As the mean values of γ^n_s are similar between the three reanalysis, same holds for the mean values of density fluxes (and also SST and SSS, not shown here) as previously found by Béranger *et al.* (1999) and Cerovečki & Mazloff (2016). The thermal component is dominant for density fluxes north of 45ºS, while the haline component leads the density changes south of 45ºS.

Differences between reanalysis γ^n_s are not in their mean pattern, but in their trends. The trends of the density thermal flux component (Fig. 5a, d and g), for all reanalysis, show two distinguish zonal regions, one with negative values from 30° to 45°S and other with positive values nearby 60°S whit the positive trends values been five times smaller than the negative values. A decreasing trend is noted with values up to -0.25 kg/m²s in the Pacific Ocean, and across western of Indian Ocean and the Brazil-Malvin Confluence. The main difference among the reanalysis is in the positive region were GODAS have the highest values between 0 and 150°E.

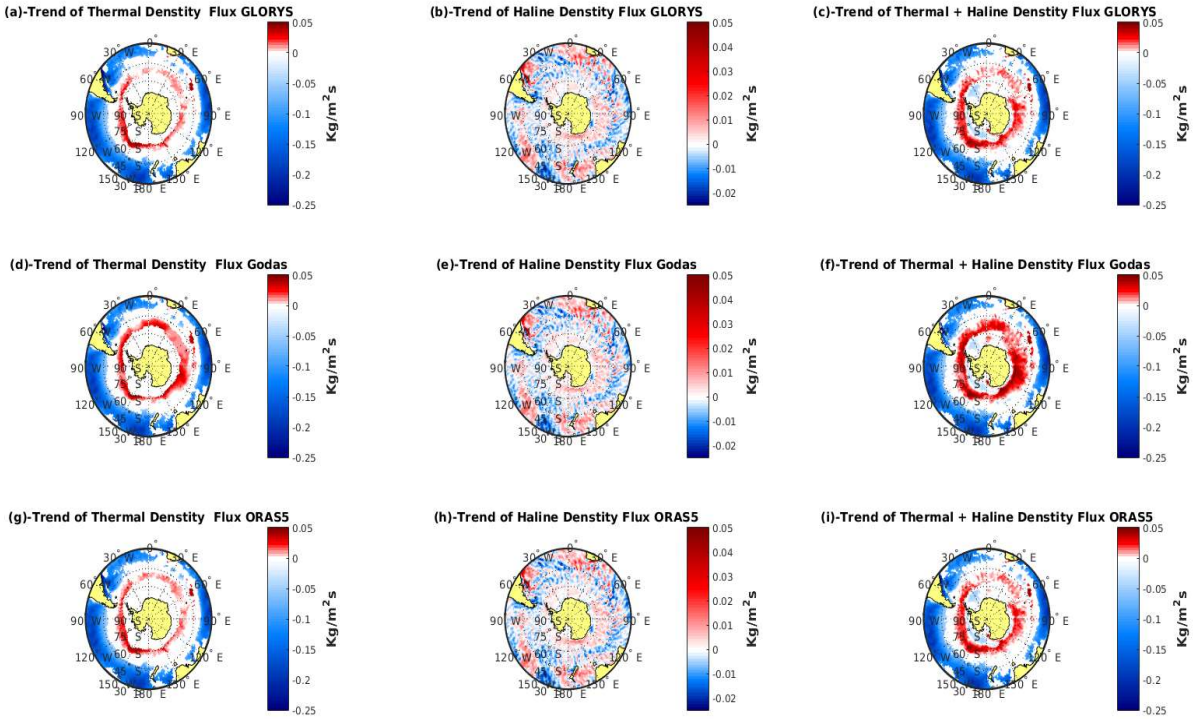

Figure 5: Trends for the: Thermal contribution of density flux (x10^{-6} kg/m^{2}s) for GLORYS, ORAS5 and GODAS reanalysis (a, d and g respectively). Haline contribution of density flux (x10^{-6} kg/m²s) for the same (b, e and h respectively). Density flux (x10^{-6} kg/m²s) for the same (c, f and i respectively). All values present in here have 95% significance.

The haline density flux for all reanalysis has a positive trend south of 60°S, indicating an increase also in the E-P over the region and negative trend between 45 and 60°S which indicates a decreased in the E-P. North of 45°S positives and negatives values of trends are found to not revealing a preferential pattern.

In general, the density fluxes for the SO are very similar to the thermal component, with the exception, conditions close to the coastal region of the Antarctic in the Amundsen and Weddell Seas. The main reason for the difference between the reanalysis γ^n_s cannot be explained by the density fluxes alone, the haline density flux are dependent on the E-P, and in the SO exists uncertainness because no direct measurements of precipitation over the ocean are available, and satellite estimates provide only a snapshot over the last decades (Trenberth; Zhang; Gehne, 2017). All reanalysis present similar mean values and trends, so differences seen it to be of temperature or salinity trends.

3.4. Sea surface temperature

Statistics between the reanalysis and the WOCE data presented in table III shows that the GLORYS reanalysis has the lowest RMSE in four out of the six sectors: sectors 1,2,4 and 6. ORAS5 perform better on the other sectors and GODAS shows the highest values of RMSE for all sectors. Considering the averaged SO, ORAS5 presents the lowest value with 0,82 and GODAS delivers a RMSE approximately 50% higher than the other datasets.

Table 3: Similar too table II for SST

		Sector 1	Sector 2	Sector 3	Sector 4	Sector 5	Sector 6	All Southern Ocean
Mean and	WOCE	10,17±9	12,34±9	10,54±9	4,70±8,88	7,08±6,3	9,57±7,87	**9,2±8,3**
Standart	GLORYS	8,67±8,7	11,97±9	10,72±9	5,68±8,77	7,52±6,4	7,67±7,67	**8,9±8,26**
Deviation	GODAS	9,18±8,4	11,34±8,3	11,28±8,8	5,58±8,43	7,25±6,3	8,03±7,64	**8,93±8,07**
	ORAS5	8,52±8,7	11,71±9	10,46±9	5,51±8,80	7,2±6,25	7,56±7,64	**8,66±8,2**
RMSE	GLORYS	0,8083	0,6735	0,8995	0.4204	0,8397	1.1012	**0,8852**
	GODAS	1,1676	1,12	1,3517	0.8383	1,0342	2.0187	**1,3962**
	ORAS5	0,92	0,7237	0,8709	0.4392	0,6439	1.0324	**0,8242**
MAPE (%)	GLORYS	-6,3	4,07	-8,41	-7.9909	0,73	107.57	**20,98**
	GODAS	1,04	22,38	-16,71	-0.02	21,69	215.67	**52,51**
	ORAS5	-3,56	1,28	-3,84	-19.50	0,80	69.27	**13,38**
r	GLORYS	0,9965	0,9981	0,9958	0.9984	0,9923	0.9901	**0,9947**
	GODAS	0,9926	0,9942	0,9907	0.9931	0,9877	0.9647	**0,9864**
	ORAS5	0,9258	0,9978	0,9960	0,9980	0,9955	0.9917	**0,9954**
Number of Points		2159	3018	6589	6485	7056	1522	**26829**

The distribution of bias (Fig. 6) indicates that, in comparison to other datasets, GODAS generally overestimates the SST, and shows higher BIAS values. Higher values are located near the coast of the Antarctic continent and the American continent. ORAS5 different from GODAS, tends to underestimate the temperature values GLORYS exhibits lower bias and values fluctuate between positive and negative depending on the region. Thus, there is not a dominant bias as the other two reanalysis.

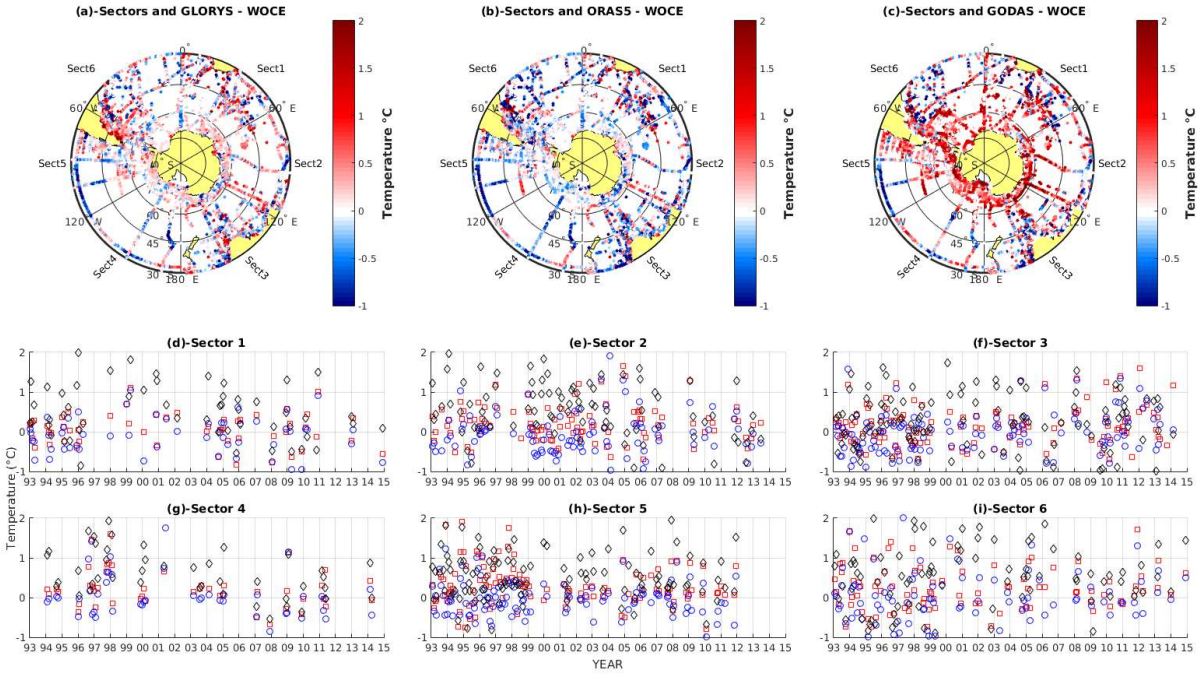

Figure 6: Same as Figure 2 but for Sea Surface Temperature.

Although temperature is the variable with the larger differences between the reanalysis and the WOCE data, it is still statistically consistent with the WOCE data for the entire Southern Ocean, except for coastal regions. As with density fluxes trends, SST trends (Fig. 7) presented by the models are very similar and agree with previous studies (Bulgin; Merchant; Ferreira, 2020; Auger *et al.*, 2021).

Trends point to a cooling in regions close to the Antarctic continent, with GODAS having a ridge strip that moves further north, mainly in the Atlantic portion of the SO. ORAS5 and GODAS consider a surface cooling to the south of 45°S in most of the SO Pacific sector and in the Weddell Sea region and in the Drake Passage. Although GLORYS also shows a negative trend in these regions they do not have statistically significant values. GODAS, as well as in density fluxes, considers more regions with significant trends that are larger, close to the Antarctic continent.

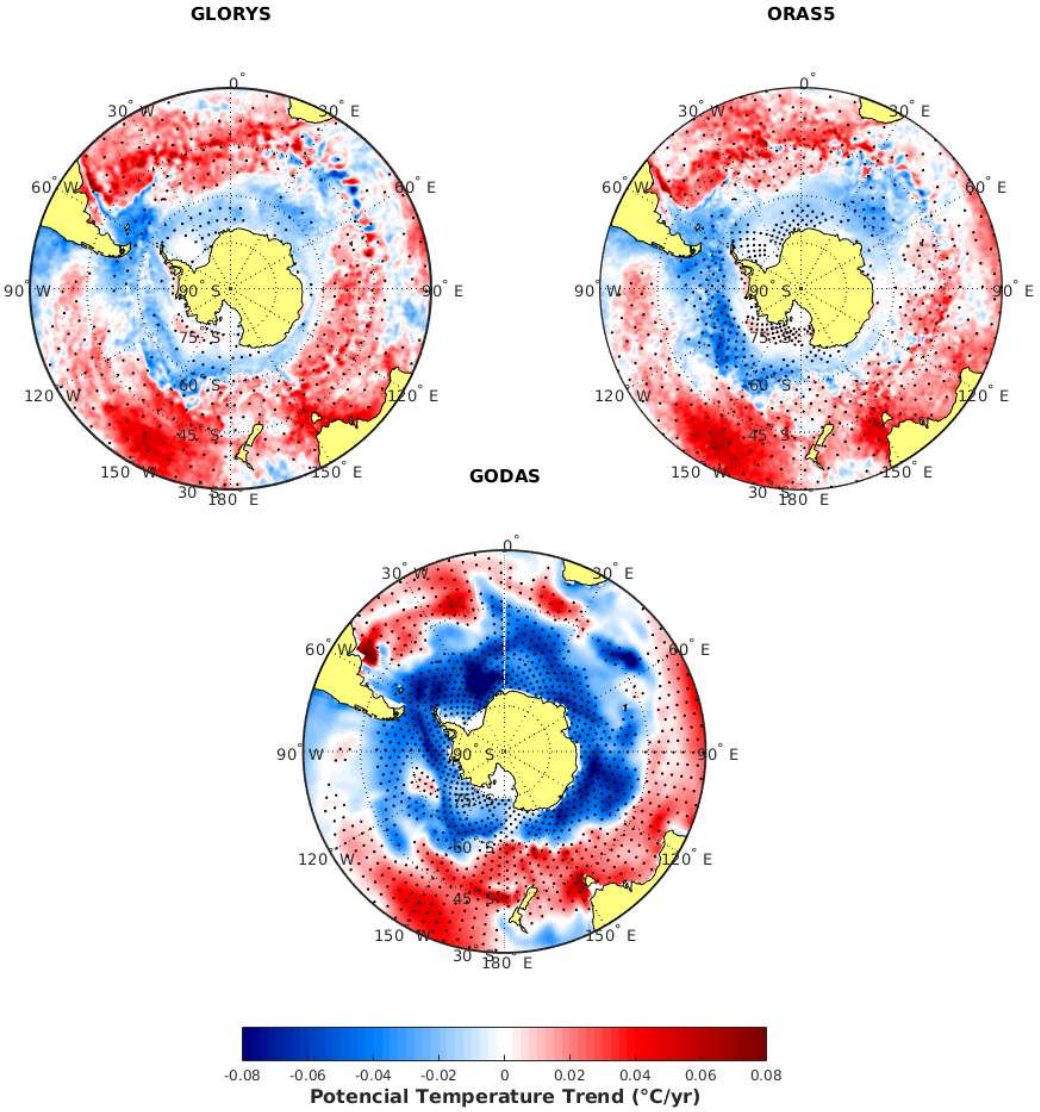

Figure 7: Same as Figure 4 but for Sea Surface Temperature.

3.5. Sea surface salinity

The SSS trend and statistics analyses (bias, RMSE, MAPE and r) calculated between the reanalysis and WOCE are very similar to the γ^n_s statistics, so they are to not show here, and focus is on SSS trends because the major difference between the reanalysis is in the γ^n_s trends and not in mean values.

GLORYS (Fig. 8a) shows an increasing salinity trend north of 45° in the SO Atlantic sector, Weddell Sea and between New Zealand and Australia. The GLORYS shows an increase in salinity north of 45, most of the Pacific sector and a decrease between 45° and 60°. The trends presented by GLORYS are very close to the results found by Aretxabaleta, Smith & Ballabrera-Poy (2015), using data from the Met Office Hadley Center – EN4 (Good; Martin;

Rayner, 2013) and the SMOS satellite (Soil Moisture and Ocean Salinity). The ORAS5 (Figure 8b) despite showing the same significant increase in the Weddell Sea and shows a slight increase salinity in the region near to New Zeland and Australia as well. It disagrees with the positive signs presented by GLORYS and found by Aretxabaleta, Smith & Ballabrera-Poy (2015) in the OS showing a decrease in salinity.

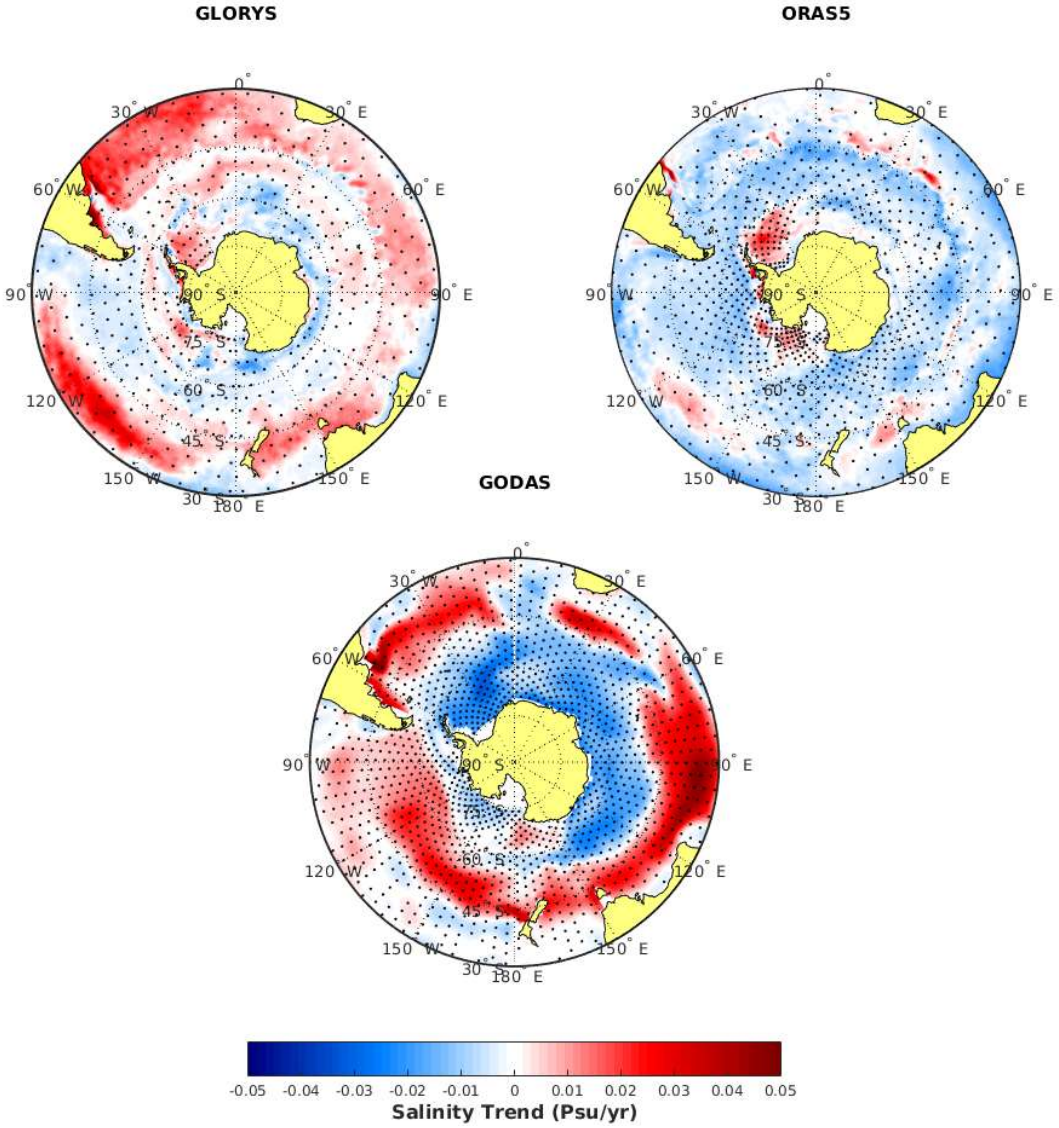

Figure 8: Same as Figure 4 but for Sea Surface Salinity.

The range of salinity trends in ORAS5 and GLORYS varies between -2 and 4 PSU. The GODAS in turn shows stronger trends ranging between -5 and 5 PSU. GODAS, unlike the other reanalysis, has a negative salinity trend in the Weddell Sea region, which is close to the results of Durak & Wijffels (2010), based on data collected in situ from different databases, between

the 1950s and 2000, and with Rye *et al.* (2020) for the period 1990 and 2014 using data from CORA5 (Cabanes *et al.*, 2013).

GLORYS and ORAS5 are similar reanalysis both in the oceanic and sea-ice models, ORAS5 used as input on T/S data derived from EN4 with XBT/MBT correction (Zuo *et al.*, 2019), while GLORYS uses data from CORA5. These two databases show distinct trends mainly in the Weddell Sea, but this is still the region where they have the closest trends. It may be argued that the differences between GLORYS and ORAS5are not due to the observational data used as an initial condition. The fact is that the ORAS5 SSS is constrained by nudging to climatology, and this may limit the SSS trends in the SO, however, more studies are needed for a definitive conclusion.

GODAS in turn, presents as initial salinity condition a synthetic salinity computed for each temperature profile using a local TS climatology, it might be noticed that it seriously underestimates salinity variability as described in http://www.cpc.ncep.noaa.gov/products/GODAS/pl/introduction_godas_web.pdf.

4. Concluding Remarks

All the reanalysis used in this study, in particular GLORYS and ORAS, demonstrated to be efficient in reproducing the WOCE data in the SO, with exception of the coastal area. They are also capable of reproducing the mean patterns of γ^n_s, SST and SSS. However, when considering the γ^n_s trends, the reanalysis differs in several points, such as the Weddell Sea, where GODAS shows a negative trend but GLORYS and ORAS5 shows a positive trend. Or across the Pacific region between 60 and 45ºS, where GODAS shows a positive trend, and the other two datasets show a negative trend.

Although GODAS seriously underestimates salinity variability as pointed out here it still shows a good representation of SST, SSS and γ^n_s. ORAS5 presents the largest differences because for the most part of the SO it shows negative trends in SSS, which in turn leads to a negative trend of γ^n_s. ORAS5 is constraint by nudging to climatology and this could be limiting the interpretation of SSS trends, but in-depth study of the impact of nudging on OS SSS trends is still needed which is beyond the scope of this work.

Finally, a better understanding of salinity trends presents a great challenge for future works, and models that study the SO, since even databases collected in situ, such as CORA5 and EN4 mentioned in the work present different trends. This is crucial for studying the impacts of the climate changes in the SST and SSS and how this modifies the MOC and the water mass formation in the SO.

Acknowledgments

The authors thank the founding support of Coordenação de Aperfeiçoamento de Pessoal de Nível Superior (CAPES; process number 88882.437121/2019-01) the E.U. Copernicus Marine Service Information, the European Centre for Medium-Range Weather Forecasts, the NCEP, the Woods Hole Oceanographic institution and the WOCE database for the data used in this work. Also, we greatly appreciate the support of ICTP through the STEP program.

Author contributions

Rafael Afonso do Nascimento Reis, lead author; Flávio Barbosa Justin, guidance, assistance in the literature review and analysis of results; Luis Felipe Ferreira de Mendonça, guidance and assistance in the literature review; Riccardo Farneti, assistance in the implementation of the methodology and analysis of results.

References

ABERNATHEY, R. P.; CEROVECKI, I.; HOLLAND, P. R.; NEWSOM, E.; MAZLOFF, M.; TALLEY, L. D. Water-mass transformation by sea ice in the upper branch of the Southern Ocean overturning. **Nat. Geosci.**, v. 9, p. 596-601, 2016.

ALMEIDA, L.; MAZLOFF, M. R.; MATA, M. M. The impact of Southern Ocean Ekman pumping, heat and freshwater flux variability on intermediate and mode water export in CMIP models: present and future scenarios. **Journal of Geophysical Research: Oceans**, v. 126, e2021JC017173, 2021. doi:10.1029/2021JC017173.

ARETXABALETA, A. L.; SMITH, K. W.; BALLABRERA-POY, J. Regime changes in global sea surface salinity trend. **Ocean Sci. Discuss.**, v. 12, 2015. doi:10.5194/osd-12-983-2015.

AUGER, M.; MORROW, R.; KESTENARE, E.; SALLÉE, J.-B.; COWLEY, R. Southern Ocean in-situ temperature trends over 25 years emerge from interannual variability. **Nat. Commun.**, v. 12, 2021. doi:10.1038/s41467-020-20781-1.

BANKS, H. T.; GREGORY, J. M. Mechanisms of ocean heat uptake in a coupled climate model and the implications for tracer-based predictions of ocean heat uptake. **Geophys. Res. Lett.**, v. 33, L07608, 2006. doi:10.1029/2005GL025352.

BEHRINGER, D.; XUE, Y. Evaluation of the global ocean data assimilation system at NCEP: the Pacific Ocean. In: SYMPOSIUM ON INTEGRATED OBSERVING AND ASSIMILATION SYSTEMS FOR ATMOSPHERE, OCEAN, AND LAND SURFACE, 8, 2004, Seattle. **Proceedings…** Seattle: American Meteorological Society, 2004.

BÉRANGER, K.; SIEFRIDT, L.; BARNIER, B.; GARNIER, E.; ROQUET, H. Evaluation of operational ECMWF surface freshwater fluxes over oceans during 1991-1997. **J. Marine Sys.**, v. 22, p. 13-36, 1999. doi:10.1016/S0924-7963(99)00028-7.

BOYER, T. P.; BARANOVA, O. K.; COLEMAN, C.; GARCIA, H. E.; GRODSKY, A.; LOCARNINI, R. A.; … ZWENG, M. M. **World Ocean Database 2018**. 2018.

BRACEGIRDLE, T. J.; SHUCKBURGH, E.; SALLEE, J.-B.; WANG, Z.; MEIJERS, A. J. S.; BRUNEAU, N.; PHILLIPS, T.; WILCOX, L. J. Assessment of surface winds over the Atlantic, Indian, and Pacific Ocean sectors of the Southern Ocean in CMIP5 models: historical bias, forcing response, and state dependence. **J. Geophys. Res. Atmos.**, v. 118, p. 547-562, 2013. doi:10.1002/jgrd.50153.

BULGIN, C. E.; MERCHANT, C. J.; FERREIRA, D. Tendencies, variability and persistence of sea surface temperature anomalies. **Sci. Rep.**, v. 10, 7986, 2020. doi:10.1038/s41598-020-64785-9.

CEROVEČKI, I.; MAZLOFF, M. R. The spatiotemporal structure of diabatic processes governing the evolution of Subantarctic Mode Water in the Southern Ocean. **J. Phys. Oceanogr.**, v. 46, p. 683-710, 2016.

DEE, D. P.; UPPALA, S. M.; SIMMONS, A. J.; BERRISFORD, P.; POLI, P.; KOBAYASHI, S.; … VITART, F. The ERA-Interim reanalysis: configuration and performance of the data assimilation system. **Quarterly Journal of the Royal Meteorological Society**, v. 137, n. 656, p. 553-597, 2011. doi:10.1002/qj.828.

DUFOUR, C.O.; GRIFFIES, S. M.; SOUZA, G. F.; FRENGER, I.; MORRISON, A. K.; PALTER, J. B.; SARMIENTO, J. L.; GALBRAITH, E. D.; DUNNE, J. P.; ANDERSON, W. G.; SLATER, R. D. Role of mesoscale eddies in cross-frontal transport of heat and biogeochemical tracers in the Southern Ocean. **Journal of Physical Oceanography**, 2015. doi:10.1175/JPO-D-14-0240.1.

DURACK, P. J.; WIJFFELS, S. E. Fifty-year trends in global ocean salinities and their relationship to broad-scale warming. **Journal of Climate**, v. 23, n. 16, p. 4342-4362, 2010.

FARNETI, R.; DOWNES, S. M.; GRIFFIES, S. M.; MARSLAND, S. J.; BEHRENS, E.; BENTSEN, M.; … YEAGER, S. G. An assessment of Antarctic Circumpolar Current and Southern Ocean meridional overturning circulation during 1958-2007 in a suite of interannual CORE-II simulations. **Ocean Modelling**, v. 93, p. 84-120, 2015. doi:10.1016/j.ocemod.2015.07.009.

FERRY, N.; PARENT, L.; GARRIC, G.; BARNIER, B.; JOURDAIN, N. Mercator global Eddy permitting ocean reanalysis GLORYS1V1: description and results. **Mercator-Ocean Q Newslett.**, v. 36, p. 15-27, 2010.

FOLDVIK, A.; GAMMELSRØD, T.; ØSTERHUS, S.; FAHRBACH, E.; ROHARDT, G.; SCHRÖDER, M.; WOODGATE, R. A. Ice shelf water overflow and bottom water formation in the southern Weddell Sea. **J. Geophys. Res.: Oceans**, v. 109, n. C2, 2004.

FOSTER, T. D.; CARMACK, E. C. Frontal zone mixing and Antarctic Bottom Water formation in the southern Weddell Sea. **Deep Sea Res. Oceanogr. Abstr.**, v. 23, n. 4, p. 301-317, 1976.

FRÖLICHER, T. L.; SARMIENTO, J. L.; PAYNTER, D. J.; DUNNE, J. P.; KRASTING, J. P.; WINTON, M. Dominance of the Southern Ocean in Anthropogenic Carbon and Heat Uptake in CMIP5 Models. **Journal of Climate**, v. 28, n. 2, p. 862-886, 2015. doi:10.1175/jcli-d-14-00117.1.

GOOD, S. A.; MARTIN, M. J.; RAYNER, N. A. EN4: quality controlled ocean temperature and salinity profiles and monthly objective analyses with uncertainty estimates. **Journal of Geophysical Research: Oceans**, v. 118, p. 6704-6716, 2013. doi:10.1002/2013JC009067.

GORDON, A. L. Bottom water formation. **Encyclopedia of Ocean Sciences**, p. 415-421, 2001. doi:10.1016/b978-012374473-9.00006-0.

GORDON, A. L.; ORSI, A. H.; MUENCH, R.; HUBER, B. A.; ZAMBIANCHI, E.; VISBECK, M. Western Ross Sea continental slope gravity currents. **Deep Sea Research Part II: Topical Studies in Oceanography**, v. 56, n. 13-14, p. 796-817, 2009. doi:10.1016/j.dsr2.2008.10.037.

JACKETT, D. R.; McDOUGALL, T. J. A neutral density variable for the world's ocean. **Journal of Physical Oceanography**, v. 27, n. 2, p. 237-263, 1997. doi:10.1175/1520-0485(1997)0272.0.CO;2.

JACOBS, S. S.; AMOS, A. F.; BRUCHHAUSEN, P. M. Ross sea oceanography and Antarctic bottom water formation. **Deep Sea Research and Oceanographic Abstracts**, v. 17, n. 6, p. 935-962, 1970. doi:10.1016/0011-7471(70)90046-x.

JUSTINO, F.; SETZER, A.; BRACEGIRDLE, T. J.; MENDES, D.; GRIMM, A.; DECHICHE, G.; SCHAEFER, C. E. G. R. Harmonic analysis of climatological temperature over Antarctica: present day and greenhouse warming perspectives. **Int. J. Climatol.**, v. 31, p. 514-530, 2011. doi:10.1002/joc.2090.

JUSTINO, F.; SILVA, A. S.; PEREIRA, M. P.; STORDAL, F.; LINDEMANN, D.; KUCHARSKI, F. The Large-Scale Climate in Response to the Retreat of the West Antarctic Ice Sheet. **Journal of Climate**, v. 28, n. 2, p. 637-650, 2015. doi:10.1175/jcli--14-00284.1.

KHATIWALA, S.; TANHUA, T.; MIKALOFF FLETCHER, S.; GERBER, M.; DONEY, S. C.; GRAVEN, H. D.; … SABINE, C. L. Global Ocean storage of anthropogenic carbon, **Biogeosciences**, v. 10, p. 2169-2191, 2013. doi:10.5194/bg-10-2169-2013.

LUMPKIN, R.; SPEER, K. Global ocean meridional overturning. **J. Phys. Oceanogr.**, v. 37, p. 2550-2562, 2007.

MARINOV, I.; GNANADESIKAN, A.; TOGGWEILER, J. R.; SARMIENTO, J. L. The Southern Ocean biogeochemical divide. **Nature**, v. 441, p. 964-967, 2006.

MARSHALL, J.; SPEER, K. Closure of the meridional overturning circulation through Southern Ocean upwelling. **Nature Geosci.**, v. 5, p. 171-180, 2012. doi:10.1038/ngeo1391.

MARSHALL, J.; SCOTT, J. R.; ARMOUR, K. C.; CAMPIN, J.-M.; KELLEY, M.; ROMANOU, A. The ocean's role in the transient response of climate to abrupt greenhouse gas forcing. **Clim. Dyn.**, v. 44, n. 7-8, p. 2287-2299, 2015. doi:10.1007/s00382-014-2308-0.

MILLARD, R. C.; YANG, K. **CTD calibration and processing methods used at Woods Hole Oceanographic Institution**. Falmouth, MA: Woods Hole Oceanographic Institution, 1993. doi:10.1575/1912/638.

NICOLAS, J. P.; BROMWICH, D. H. Precipitation changes in high southern latitudes from global reanalysis: a cautionary tale. **Surv. Geophys.**, v. 32, p. 475-494, 2011. doi:10.1007/s10712-011-9114-6.

ORSI, H.; WHITWORTH, T.; NOWLIN JR, W. D. On the meridional extent and fronts of the Antarctic Circumpolar Current. **Deep Sea Research Part I: Oceanographic Research Papers**, v. 42, p. 641-673, 1995.

PEIXOTO, J. P.; OORT, A. H. **Physics of climate**. New York, NY: American Institute of Physics, 1992.

PELLICHERO, V.; SALLÉE, J.-B.; CHAPMAN, C. C.; DOWNES, S. M. The Southern Ocean meridional overturning in the sea-ice sector is driven by freshwater fluxes. **Nat. Commun.**, v. 9, p. 1789, 2018. doi:10.1038/s41467-018-04101-2.

RINTOUL, S. R. On the origin and influence of Adélie land bottom water. In: JACOBS, S.; WEISS, R. (Eds.). **Ocean, ice, and atmosphere**: interactions at the Antarctic Continental margin. Washington: American Geophysical Union, 1998. p. 151-171. (Geophysical Monograph Series, 75).

RINTOUL, S. R. The global influence of localized dynamics in the Southern Ocean. **Nature**, v. 558, p. 209-218, 2018. doi:10.1038/s41586-018-0182-3.

RYE, C. D.; MARSHALL, J.; KELLEY, M.; RUSSELL, G.; NAZARENKO, L. S.; KOSTOV, Y., … HANSEN, J. Antarctic glacial melt as a driver of recent Southern Ocean climate trends. **Geophysical Research Letters**, e2019GL086892, 2020. doi:10.1029/2019gl086892.

SABINE, C. L.; FEELY, R. A.; GRUBER, N.; KEY, R. M.; LEE, K.; BULLISTER, J. L.; … RIOS, A. F. The oceanic sink for anthropogenic CO2. **Science**, v. 305, n. 5682, p. 367-371, 2004. doi:10.1126/science.1097403.

SALLÉE, J.-B.; SHUCKBURGH, E.; BRUNEAU, N.; MEIJERS, A. J. S.; BRACEGIRDLE, T. J.; WANG, Z.; ROY, T. Assessment of Southern Ocean water mass circulation and characteristics in CMIP5 models: historical bias and forcing response. **J. Geophys. Res. Oceans**, v. 118, p. 1830-1844, 2013. doi:10.1002/jgrc.20135.

SARMIENTO, J. L.; GRUBER, N.; BRZEZINSKI, M. A.; DUNNE, J. P. High-latitude controls of thermocline nutrients and low latitude biological productivity. **Nature**, v. 427, p. 56-60, 2004.

SCHMITT, R. W.; BODGEN, P. S.; DORMAN, C. E. Evaporation minus precipitation and density fluxes for the North Atlantic. **J. Phys. Oceanogr.**, p. 1208-1221, 1989.

SCHNEIDER, D. P.; REUSCH, D. B. Antarctic and Southern Ocean Surface Temperatures in CMIP5 Models in the Context of the Surface Energy Budget. **Journal of Climate**, v. 29, n. 5, p. 1689-1716, 2016.

SILVANO, A. Changes in the Southern Ocean. **Nat. Geosci.**, v. 13, p. 4-5, 2020. doi: 10.1038/s41561-019-0516-2.

SLOYAN, B. M.; RINTOUL, S. R. The Southern Ocean limb of the global deep overturning circulation. **J. Phys. Oceanogr.**, v. 31, p. 143-173, 2001.

SOUZA, J. M. A. C.; COUTO, P.; SOUTELINO, R.; ROUGHAN, M. Evaluation of four global ocean reanalysis products for New Zealand waters: a guide for regional ocean modelling. **New Zealand Journal of Marine and Freshwater Research**, v. 55, n. 1, p. 132-155, 2021. doi:10.1080/00288330.2020.1713179.

TALLEY, L. D.; PICKARD, G. L.; EMERY, W. J.; SWIFT, J. H. **Descriptive physical oceanography**: an introduction. 6. ed. Boston: Elsevier, 2011. 560 p.

TRENBERTH, K. E.; ZHANG, Y.; GEHNE, M. Intermittency in precipitation: duration, frequency, intensity, and amounts using hourly data. **J. Hydrometeor.**, v. 18, p. 1393-1412, 2017. doi:10.1175/JHM-D-16-0263.1.

UPPALA, S. M.; DEE, D. P.; KOBAYASHI, S.; SIMMONS, A. J. Evolution of reanalysis at ECMWF. In: WCRP International Conference on Reanalysis, 3, 2008, Tokyo, Japan. **Proceedings…** Tokyo, Japan, 2008.

WATSON, A. J.; NAVEIRA GARABATO, A. C. The role of Southern Ocean mixing and upwelling in glacial-interglacial atmospheric CO2 change. **Tellus B**, v. 58, p. 73-87, 2006. doi:10.1111/j.1600-0889.2005.00167.x.

WILLIAMS, G. D.; AOKI, S.; JACOBS, S. S.; RINTOUL, S. R.; TAMURA, T.; BINDOFF, N. L. Antarctic bottom water from the Adélie and George V Land coast, East Antarctica (140-149°E). **J. Geophys. Res.**, v. 115, C04027, 2010.

YAMAMOTO, A.; ABE-OUCHI, A.; SHIGEMITSU, M.; OKA, A.; TAKAHASHI, K.; OHGAITO, R.; YAMANAKA, Y. Global deep ocean oxygenation by enhanced ventilation in the Southern Ocean under long-term global warming. **Global Biogeochem. Cycles**, v. 29, p. 1801-1815, 2015. doi:10.1002/2015GB005181.

YU, L. S.; JIN, X. Z.; WELLER, R. A. **Multidecade global flux datasets from the objectively analyzed air-sea fluxes (OAFlux) project**: latent and sensible heat fluxes, ocean evaporation, and related surface meteorological variables. Falmouth, MA: Woods Hole Oceanographic Institution, 2008. 64 p. (OAFlux Project Technical Report).

ZUO, H.; BALMASEDA, M. A.; TIETSCHE, S.; MOGENSEN, K.; MAYER, M. The ECMWF operational ensemble reanalysis–analysis system for ocean and sea ice: a description of the system and assessment. **Ocean Sci.**, v. 15, p. 779-808, 2019. doi:10.5194/os-15-779-2019.

ARTIGO 2

Southern Ocean heat content and its link to Large-scale climate based on reanalyses datasets

Rafael Afonso do Nascimento Reis[1]*, Flávio Barbosa Justino[2], Luís Felipe Ferreira de Mendonça[3] & Riccardo Farneti[4]

Abstract: Global oceans are an important regulator of the global climate, and the Southern Ocean (SO) is responsible for most of the anthropogenic CO2 and heat uptake. Over the years many studies focused on the variation of the heat content, formation and physicochemical properties of water masses produced in the SO. The present work contributes by analyzing dominant patterns of the Ocean Heat Content (OHC) as delivered by three oceanic reanalyses, namely: GLORYS, ORAS5 and GODAS and the IAP database. All data show an increase in the total OHC across the SO with GLORYS having the largest positive trend by up $1{,}38x10^{18}$ J/yr whereas GODAS shows the lowest with $6{,}2x10^{17}$ J/yr. GLORYS, ORAS5 and IAP first variability mode are substantially associated with ENSO and presents the Antarctic Dipole feature. The second mode is more linked to oceanic eddies well represented by GLORYS and ORAS5. Only GLORYS and ORAS5 show a significant correlation with SAM, also forming the Antarctic Dipole, but with a sign opposite to that of ENSO. Although this characteristic of linkage between SAM and OHC is already known it has been noted that with the removal of the ENSO signal SAM ceases to play a significant role in the Pacific Ocean indicating that SAM acts only as a softener of ENSO impacts in the Pacific Ocean. Both models, MOM025 and MOM, due to the fact that they rule out the interaction of ENSO in the Southern Ocean, fail to represent the variability of the OHC in this one.

Keywords: Reanalysis; GODAS; GLORYS; ORAS5; SAM; ENSO; CORE-II.

1. Introduction

The global oceans exchange with the atmosphere heat, gases, and momentum thus regulating the global climate. Oceanic regions are responsible for absorbing about 93% of the excessive energy derived from global warming (Rhein; Rintoul; Aoki, 2013). One of the most critical regions of the global ocean is the Southern Ocean (SO) which here is assumed to be southward to 30ºS. This region is unique in its features because it connects all oceanic basins

[1] rafael_cgb@hotmail.com, https://orcid.org/0000-0003-4115-2265, Universidade Federal de Viçosa – Departamento de Engenharia Agrícola – Sala 107 – ZIPCODE: 36570-900 – Viçosa – Minas Gerais – Brasil.

[2] fjustino@ufv.br, https://orcid.org/0000-0003-0929-1388, Universidade Federal de Viçosa – Departamento de Engenharia Agrícola – Sala 107 – ZIPCODE: 36570-900 – Viçosa – Minas Gerais – Brasil.

[3] luis.mendonca@ufba.br, https://orcid.org/0000-0001-7836-200X, Universidade Federal da Bahia – Instituto de Geociências – Departamento de Oceanografia – Rua Barão de Jeremoabo, s/n – Campus Universitário de Ondina – ZIPCODE: 40170-020 – Salvador – Bahia – Brasil.

[4] rfarneti@ictp.it, https://orcid.org/0000-0001-7781-6436, ICTP – Earth System Physics Section – Strada Costiera, 11 – ZIPCODE: 34151 – Trieste – Italy.

* Corresponding author: Rafael Afonso do Nascimento Reis - Tel: +55 (55) 99129-1355 - Address: Universidade Federal de Viçosa – Departamento de Engenharia Agrícola – Sala 107 – ZIPCODE: 36570-900 – Viçosa – Minas Gerais – Brasil. e-mail address: rafael_cgb@hotmail.com.

transporting water from one basin to another through the Antarctic Circumpolar Current (ACC). The SO is relevant to ocean ventilation, because its water masses transport heat and gases to the global ocean in different depths (Sloyan & Rintoul, 2001; Marinov *et al*., 2006; Sarmiento *et al*., 2004; Marshall & Speer, 2012; Farneti *et al*., 2015, among others). The SO is also a crucial part of the Meridional Overturning Circulation – MOC (Sloyan & Rintoul, 2001); Lumpkin & Speer, 2007; Marshall & Speer, 2012; Abernathey *et al*., 2016; Pellichero *et al*., 2018; Rintoul, 2018).

Recent studies have demonstrated that the SO absorbs by about 40-50% of anthropogenic carbon dioxide – CO_2 (Sabine *et al*., 2004; Watson & Naveira Garabato, 2006; Frölicher *et al*., 2015, among others), and uptakes more than 70% of the heat-related activities (Dufour *et al*., 2015; Frölicher *et al*., 2015). However, the SO is poorly sampled, and accurate modeling results are scarce (Silvano, 2020) which leads to many questions about processes occurring in surface, sub-surface and interior waters (Farneti *et al*., 2015). Indeed, a recent study across different ocean basins aiming at understanding the oceanic heat content (OHC), found large discrepancies of OHC in different layers of the Southern Ocean which subsequently led to misrepresentation of oceanic convection (Wang *et al*., 2018). Moreover, it is crucial to reproduce main processes related to the SO OHC and their variability, because they exert a major role for improving ocean and coupled modeling parameterization resulting in more reliable past, present and future climates (Griffies *et al.*, 2005; Schuckmann *et al*., 2016).

In recent years many studies have been conducted to evaluate ocean models and reanalysis focusing on a satisfactory representation of complex processes that occur in the SO (Justino *et al*., 2011; Bracegirdle *et al*., 2013; Sallée *et al*., 2013; Farneti *et al*., 2015; Justino *et al*., 2015; Wang & Dommenget, 2015; Schneider & Reusch, 2016; Wang *et al*., 2018; Almeida; Mazloff; Mata, 2021; Justino *et al*., 2019). Following a similar path, this work aims to analyze high and medium resolution reanalysis: (1) GLORYS2v4 – Global Ocean Reanalysis and Simulations 2v4 - here after GLORYS (Ferry *et al*., 2010); (2) ORAS5 – Ocean ReAnalysis System 5 (Zuo *et al*., 2019); and (3) GODAS – Global Ocean Data Assimilation System (Behringer & Xue, 2004) to verify their capability to represent the OHC vertical profile and its variability in the SO.

Reanalysis have been used as initial and boundary conditions in all sort of modelling experiments. Large effort has been applied to characterize the temporal and spatial reliability of these data with respect to in situ observations. However, most studies deal with atmospheric variables. Therefore, reanalysis have to be analyzed not only on their capability to reproduced atmospheric conditions but also oceanic features at surface and sub-surface layers. This study

aims to analyzing 4 datasets under different horizontal resolutions in their mean conditions and variability. As well as we focus on the link among the OHC, dominant climate modes and atmospheric conditions. Finally, a regional oceanic modelling experiment conducted with the MOM is analyzed to verify the model capability to reproduce reanalysis data.

2. Methodology

2.1. Ocean reanalyses

Three monthly averaged oceanic reanalyses, between the years 1993 and 2014 are applied. All reanalysis has atmospheric forcing data from European Center for Medium-Range Weather Forecasts (ECMWF) 'Interim' reanalysis (ERAI; Uppala *et al*., 2008; Dee *et al*., 2011). The GLORYS2V4 hereafter called (GLORYS) is an oceanic reanalysis that runs with the model NEMO 3.1 and the ice model LIM2, with a horizontal resolution of 1/4° by 1/4° and 75 vertical levels – https://www.mercator-ocean.fr/en/ocean-science/glorys/ (Garric *et al*., 2017). It includes assimilation of a long track altimeter observations (sea level anomaly), satellite sea surface temperature (SST), sea ice concentration and in situ temperature and salinity vertical profiles from the 'Coriolis Ocean database ReAnalysis' (CORA) dataset (Souza *et al*., 2021).

The European Centre for Medium-Range Weather Forecasts (ECWMF) Ocean ReAnalysis System 5 (ORAS5) also applies NEMO model, but your version 3.4.1 uses the LIM2 as an ice model, with a horizontal resolution of 25 km on tropics which increases to 9 km in polar regions, with 75 vertical levels – https://www.ecmwf.int/en/forecasts/dataset/ocean-reanalysis-system-5 (Zuo *et al*., 2019). ORA5 Differences between ORA5 and GLORYS also arise from the sea surface salinity (SSS) calculation, which is constraint by nudging to climatology. The last model is the NCEP (National Centers for Environmental Prediction) Global Ocean Data Assimilation System (GODAS) which runs with the oceanic model GFDL MOM.v3 with a horizontal grid of 1° longitude by 1/3° latitude, 40 vertical levels (Behringer & Xue, 2004), his salinity initial conditions is a synthetic salinity computed for each temperature profile using a local TS climatology.

We also utilized the Institute of Atmospheric Physics (IAP) OHC data – ftp://www.ocean.iap.ac.cn/cheng/IAP_Ocean_heat_content_0_2000m/ (Cheng *et al*., 2017). This dataset is generated by XBT profiles corrected by using the CH14 scheme (Cheng & Zhu, 2014) with a horizontal resolution of 1° by 1°, and 41 vertical levels from 1- to 2000-m depths.

2.2. Oceanic modelling experiments

The two annual mean global ocean-sea ice models utilized in this work are:

- Geophysical Fluid Dynamics Laboratory - Modular Ocean Model (GFLD-MOM) which participated in the Coordinated Ocean-sea ice Reference Experiments phase II – CORE-II (Danabasoglu *et al*., 2014) with 1° resolution and the codes of Griffies *et al*. (2011).
- GFDL-MOM025 derived from GFDL-MOM but with 1/4° resolution at the equator reaching 9 km at 70°N/S used as the oceanic component in Delworth *et al*. (2012) based on the MOM5 ocean model (Griffies *et al*., 2012).

Both models are forced by atmospheric data from the CORE-II from 1948 to 2007 (Large & Yeager, 2009) and run 5 repeated cycles with atmospheric forcing, with the first 4 being considered spin-ups. Although the models have a period of 60 years in this work, they will only be analyzed from the period 1993 to 2007 where it overlaps with the other databases used. It is important to emphasize that the wind stress data are not directly applied to the models but calculated through bulk formula and through wind speed and surface ocean currents simulated by the models themselves. If the reader is interested in a more detailed description of both models, see Appendix B by Farneti *et al*. (2015).

2.3. Climate indexes

In order to evaluate the impact of large-scale climate indices and teleconnections in the OHC, the El Niño South Oscillation (ENSO) and Southern Annular Mode (SAM) have been chosen. This is reasonable, because these indices induce changes in the atmospheric circulation that modifies the oceanic wind-driven circulation, in particular the ACC (Farneti *et al.,* 2015). The ENSO and SAM timeseries have been acquired at https://origin.cpc.ncep.noaa.gov/products/analysis_monitoring/ensostuff/ONI_v5.php, and https://www.cpc.ncep.noaa.gov/products/precip/Cwlink/daily_ao_index/aao/monthly.aao.index.b79.current.ascii, respectively. It has to be mentioned that no significant differences have been noticed by using the Nino 3.4 index instead of the ONI applied herein.

2.4. Ocean heat content

In this study, the Ocean Heat Content in the 0-300 layer (OHC, hereafter) is calculated from equation 1, as used by Stephenson, Gille & Sprintall (2012).

$$OHC = \int_0^{300} \rho C_p T dz \qquad \text{Eq. (1)}$$

Where, ρ, C_p and T are the density of seawater, thermal capacity. and potential temperature respectively. The density of seawater and the thermal capacity was calculated utilizing the matlab package Gibbs-SeaWater (GSW) Oceanographic Toolbox (McDougall & Barker, 2011), available at http://teos-10.org/software.htm for Matlab. The total OHC (OHC_t) is calculated by the followed equation (Meyssignac *et al.,* 2019):

$$OHC_t = \iint OHC\, dxdy \qquad \text{Eq. (2)}$$

3. Results

3.1 Ocean heat content

All databases exhibit positive OHC trends but with distinct magnitudes, GODAS might be highlighted because shows an OHC trend 10 times lower than the others (Table 1). Two trends have been computed with and without the seasonal cycle, and results show that conditions which departure from seasonality increase substantially the trend magnitude. Therefore, recent Southern Hemisphere warning is an important candidate to be responsible for the temporal increase of OHC in the SO. Among analyzed data, the IAP shows total trends higher than those shown by the reanalysis. However, this data with is more related with observations show remarkable influence of seasonality, because when this is removed trends are in order of those delivered by reanalysis (Table 1).

Table 1: Mean, standard deviation and trend for the Total Ocean Heat Content and trend for the monthly anomaly

	Mean	**Std**	**Total Trend**	**Trend with removed seasonal cycle**
IAP	1,26 x 10^{21} J	6,4 x 10^{19} J	1 x 10^{18} J/y	1,36 x 10^{18} J/y
GLORYS	1,29 x 10^{21} J	1,2 x 10^{20} J	7,28 x 10^{17} J/y	1,38 x 10^{18} J/y
ORAS5	1,25 x 10^{21} J	1,28 x 10^{20} J	5,26 x 10^{17} J	1,23 x 10^{18} J/y
GODAS	9,2 x 10^{20} J	4,5 x 10^{19} J	3,75 x 10^{17} J	6,2 x 10^{17} J/y

The GLORYS, ORAS and IAP reanalysis have a close trend (Table 1), with GLORYS showing the highest value, 1,38x10^{18} J/yr, GODAS trend is approximately half of the others. A correlation was made between the OHC_t anomalies and the SAM, NINO34 to verify whether

those modes of variability are in line with trends previous shown. It is pointed out that all correlations were not statistically significant up to a 6-month lag period.

The temporal evolution of the OHC, as reproduced by spatially-vertically averaged monthly anomalies by the three reanalysis show values varying from 3 to $3x10^{19}$ J (Fig. 1). Large differences among those data occur early 2000s where the reanalysis show a shift from negative to positive values. It is important to notice that ORA5 matches closely the IAP evolution. But from 2000 to 2010 an out-of-phase relationship is evident between the IAP and reanalysis; 2010 onward those data show in-phase evolution (Fig. 1) showing that the climate forcing is more similarly captured/assimilated by the reanalysis oceanic models. The upward trend in OHC in the OS, also shown in other studies (Cheng *et al*., 2017; Sallée, 2018; Wang *et al.*, 2018), it is crucial to shed light on the processes of sea ice formation (Martinson, 1990) and in the acceleration of Antarctic ice melting (Schmidtko *et al*., 2014). It has been demonstrated that advection of mid-latitudes warm waters has the capability to modify the temporal and spatial sea ice variability (Eayrs *et al*., 2019).

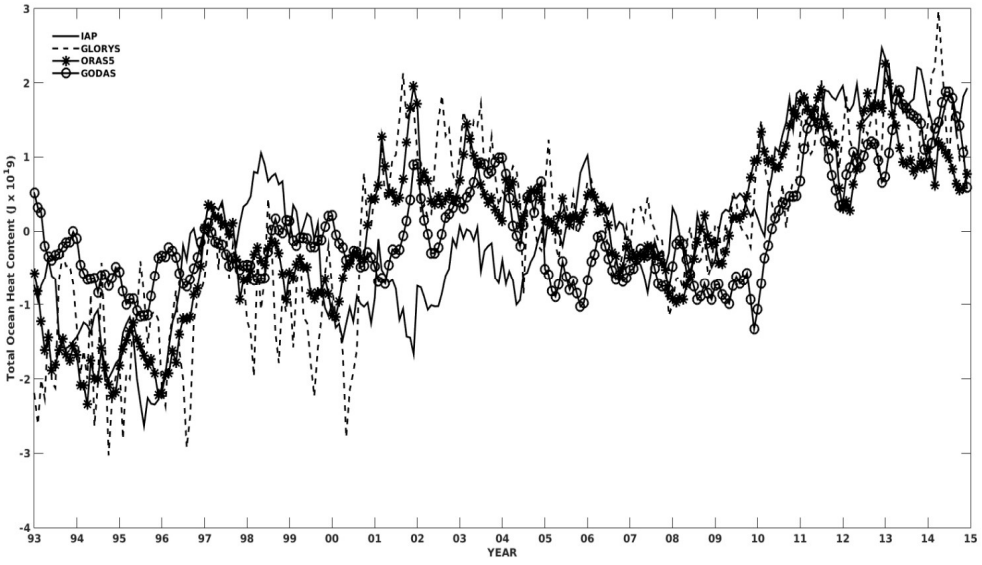

Figure 1: Monthly anomaly of the Southern Ocean Total Ocean Heat Content (10^{19} J) for the IAP, GLORYS, ORAS5, and GODAS.

Negative OHC_t anomalies during the 2000-2011 interval have also been found by Landschützer *et al*. (2015) and Keppler & Landschützer (2019). The authors argue that in the period the SO experienced more intense zonal winds over the South West Pacific sector and weaker over the Atlantic and Indian sectors. This pattern has led to an increase in subsidence in the Atlantic sector and a warmer surface, while in the Pacific sector and increase in upwelling

leads to cooler surfaces. This decrease in SST in the Pacific sector generates the drop in OHC in the referred period. It may be reasonably claimed that the IAP temporal evolution pattern, is related to the number of XBT samples because it is highly dependent on total observations and in situ collections. The reanalysis are supplied by different types of measures and remote sensing which are gridded distributed across the SO.

Figure 2 shows the spatial trends distribution. The IAP, ORAS5, and GLORYS have similar OHC trends, GODAS shows similarities with the others, but is the one that most differs among all, especially in the Pacific and Indian sectors. Across the South East region of the Pacific sector, the IAP presents a negative trend region more similar to the GLORYS and ORAS5. However, in 45ºS IAP disagrees with GLORYS and ORAS5. The IAP data shows a region of a positive trend that advances until approximately 90°W. GLORYS and ORAS5 have the same positive region but it advances close to the American continent. Similar feature is found in the temperature trends by Armour *et al.* (2016). GODAS, in turn, does not present this region with a positive trend and overestimates the negative trend in the Pacific Ocean.

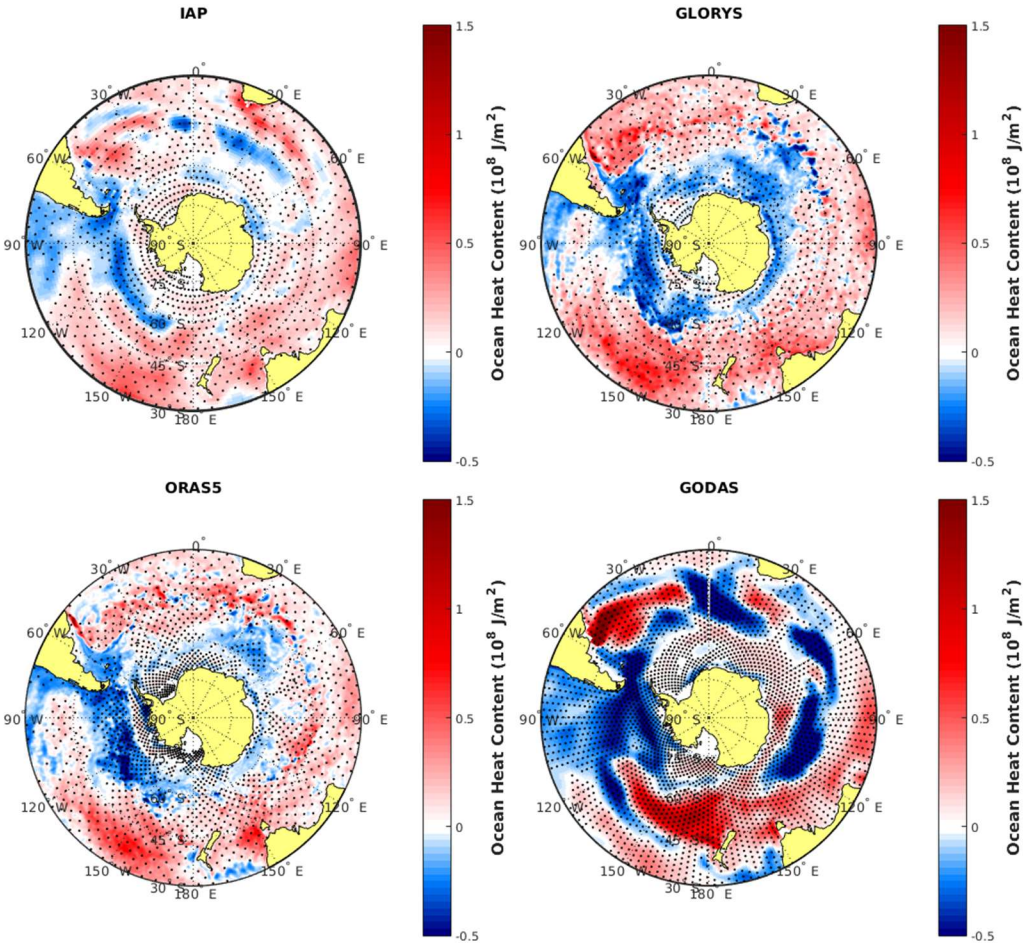

Figure 2: OHC trend for the IAP, GLORYS, ORAS5, and GODAS. Regions with statistical significance at 95% are dotted.

This region, eastern of the Pacific Ocean is a key region for the formation of the SAMW (McCartney, 1977, 1982), in association with the AAIW, they are crucial for ventilating the northern intermediate layers of the subtropical gyres (Garabato *et al*., 2009). The decreasing trend in OHC may reproduce drop in water temperatures generated in this region, observed between 1990 and 2005 by Schneider *et al*. (2005) and Garabato *et al*. (2009).

GLORYS and ORAS5 have similar trends pattern with an increase/decrease in the OHC north/south of the ACC, with positive regions near the Antarctic continent, in agreement with previous temperature trend studies (Armour *et al*., 2016; Auger *et al*., 2021; to cite a few). This heating pattern have been associated to changes in the MOC, where increases in heat uptake resulting from anthropogenic activities, are balanced by anomalies of northward heat transport (Armour *et al*., 2016). The decrease/cooling in GLORYS and ORAS5 OHC, on the other hand, is consistent with the multidecadal trend in the SO since 1979, until the period of this work from 1993 until 2014 (Fan; Deser; Schneider, 2014; Armour & Bitz, 2015; Lecomte *et al*., 2017). This has also been related to increased Antarctic sea-ice area, as previously found (Vaughan *et al*., 2013).

The IAP overestimates regions with positive trends near the Antarctic continent whereas GODAS displays characteristics that resemble an OHC more responsive to meso-scale process, rather than associated to the zonal westerly atmospheric flow. The lack of observations in both spatial and temporal distributions and the fact that most observations in the region are in summer result in a mismatch between the IAP and other reanalysis (Sallée, 2018). The variability of the upper ocean is also driven by surface forcing's, advection, through eddies and frontal meanders, which can also cause warming or cooling in the upper ocean (Joyce *et al.*, 1981). Oceanic eddies in addition play an important role on the exchange of heat and gas in the ocean-atmosphere interface (Martínez-Moreno *et al.*, 2021; Pezzi *et al.*, 2021). The eddy contribution is locally incorporated in the IAP when available. It has to me mentioned that due to the crucial influence of this region in todays and future climates, much effort has to be made involving field work, modeling and satellite derived-data to have an extensive representation of climate variables across the challenging Southern Ocean region.

3.2. OHC (Empirical Ortogonal Function)

Further analyses to shed light on the OHC temporal and spatial variability are conducted by using Empirical Orthogonal Function – EOF (Fig. 3 and 5). The first 2 EOFs explain more

than 50% of the variance in the OS. The first EOF (Fig. 3) delivers very similar pattern between GLORYS and ORAS5 highlighting the Antarctic dipole with negative (positive) values in the Pacific (Atlantic) Ocean, in line with Wang & Dommenget (2015). The IAP shows large positive anomalies in the Indian Ocean at 45°S and barely reproduces the dipole, as found in GLORYS and ORAS5. GODAS on the other hand, displays a different structure and in most locations disagree to the other reanalysis. These differences among the reanalysis may be a result of ocean eddies representations since GLORYS and ORAS5 are based on the same ocean model, which is eddy-permitting and gives a better description of more turbulent regions, such as ACC. The IAP shows drawbacks over regions where eddies are an important component (Cheng *et al*., 2017). The reanalysis also varies in terms of the amount explained variance. The 1st mode is more relevant in GODAS indicating that large scale patterns which changes smoothly, dominate the temporal variability. In opposite to what has been delivered by GLORYS and ORAS5, showing that high frequency events play an important role.

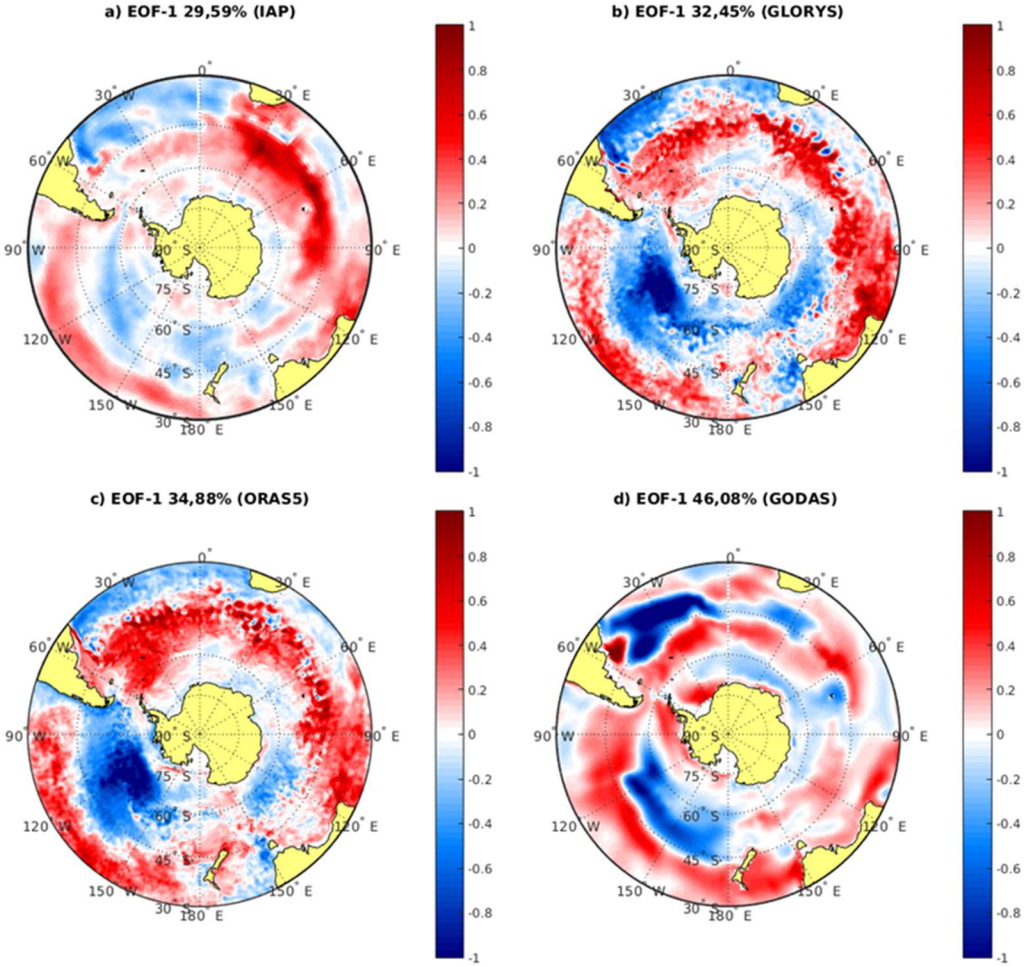

Figure 3: First EOF for the IAP (a), GLORYS (b), ORAS5 (c) and GODAS (d). The values in the heading are the explained variance for each dataset. All the values have been normalized for a better comparison.

By analyzing the 1st principal component time series (not shown), it is found that GLORYS, ORAS5, and IAP run mostly at same pace, while GODAS along the temporal interval delivers opposite value, after 2009. Correlations between ENSO events and the PC-1 (Table 2) shows highly and significant negatively correlated values (by up to -0.66) for GLORYS and ORAS5, lower values are found for IAP and GODAS. The ENSO index leads maximum correlation by three and four months though its influence is noticed throughout 6 months.

The out-of-phase variability between ENSO and the OHC dominant pattern, indicates that the amount of heat content is modified along the 40-60°S latitudinal belt and in the vicinity of Antarctic peninsula, because of changes in the position of the polar and subtropical jet. Turning to SAM evaluations, it is demonstrated that correlation values are lower with respect to ENSO (by up to 0.3) and are not significant for IAP and GODAS. It is important to highlight those positive values of the SAM, which are dominated by increased atmospheric pressure over mid-latitudes, induces and vice-versa is coupled to OHC.

Table 2: Correlation between ENSO/SAM and the PC-1

		Lag 0	**Lag 1**	**Lag 2**	**Lag 3**	**Lag 4**	**Lag 5**	**Lag 6**
ENSO	IAP	-0,2944	-0,2973	-0,295	-0,2898	-0,2803	-0,2644	-0,2432
	GLORYS	-0,5292	-0,5844	-0,6220	-0,6406	-0,6385	-0,6136	-0,5649
	ORAS5	-0,4918	-0,5675	-0,6240	-0,6569	-0,6630	-0,6418	-0,5952
	GODAS	-0,1736	-0,1682	-0,1609	-0,1535	-0,1471	-0,143	-0,1416
SAM	IAP	*0,1110	*0,1121	*0,1023	*0,0905	*0,0998	*0,1078	*0,1066
	GLORYS	0,2231	0,2816	0,2840	0,2989	0,2785	0,2424	0,2256
	ORAS5	0,1859	0,2831	0,3063	0,3074	0,2856	0,2369	0,2279
	GODAS	*0,0307	*0,0243	*0,0208	0,0178	*0,0245	*0,0297	*0,0332

Note: The lag correlation assumes that the ENSO and SAM lead. Values marked with * are not statistically significance.

The PC-1 power spectral distribution (PDS) (Fig. 4) primary indicates the characteristic red noise feature. A dominant peak is delivered by ORAS5 and GLORYS that ranges from 5 to 7 years, however, IAP and GODAS do not show similar pattern. The 5-7 years periodicity is tightly linked to ENSO. The absence of this signal in IAP and GODAS reveals that teleconnections arising from equatorial dynamics are absent or very weak in these datasets.

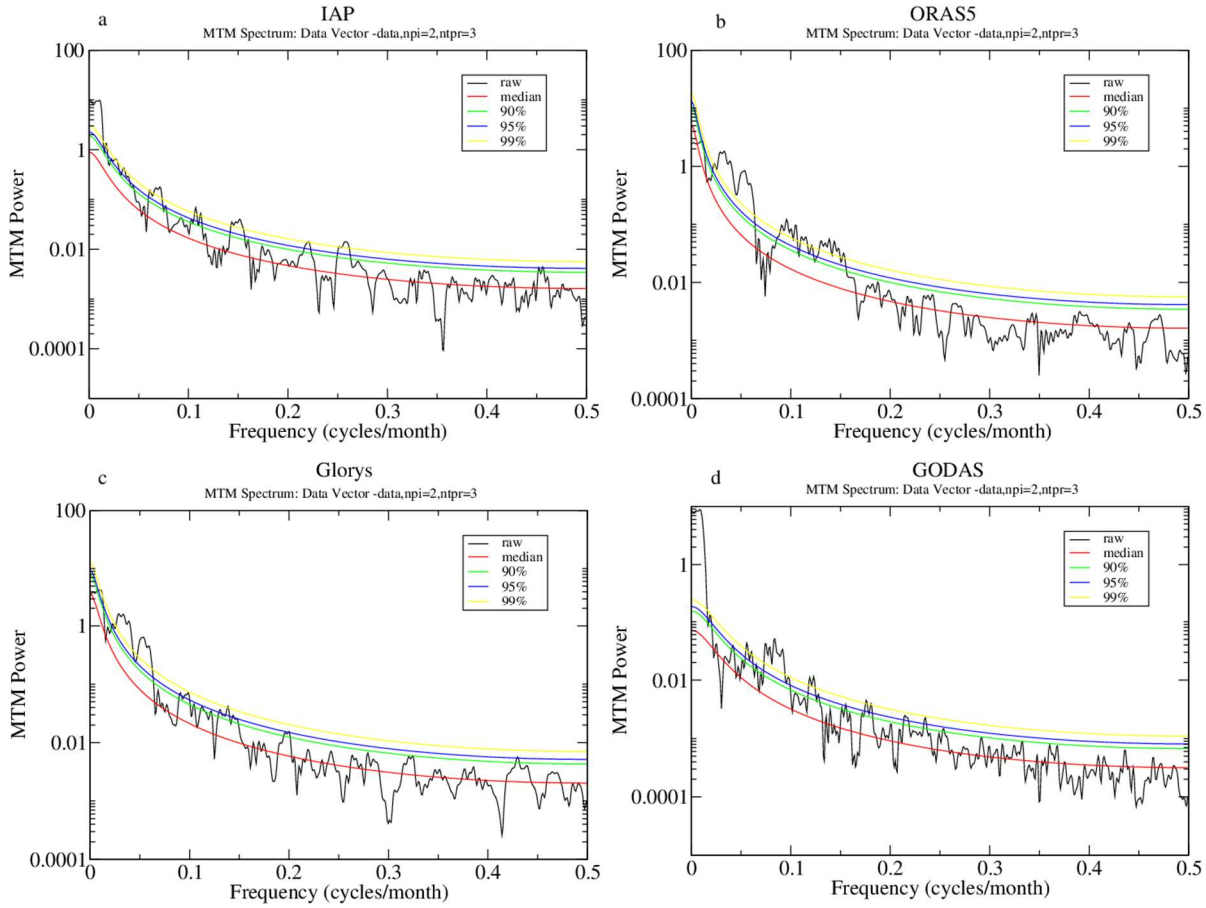

Figure 4: Power spectral of OHC 1st principal component based on multi-taped method for IAP (a), ORAS5(b), GLORYS(c) and GODAS(d).

The second component of the EOF (Figure 5a-d) shows main discrepancies between the data. GLORYS and ORAS5 present a wave pattern around the Antarctic continent at 45ºS like what was found previously for the SST by Wang & Dommenget (2015). The IAP also has this wave, but it has a weaker representation on the downside across the Indian Ocean. The GODAS reanalysis does not show the wave train around the continent and attains values in opposite to other reanalysis in several regions, such as the positive anomaly in the Pacific sector, while all others show a negative anomaly.

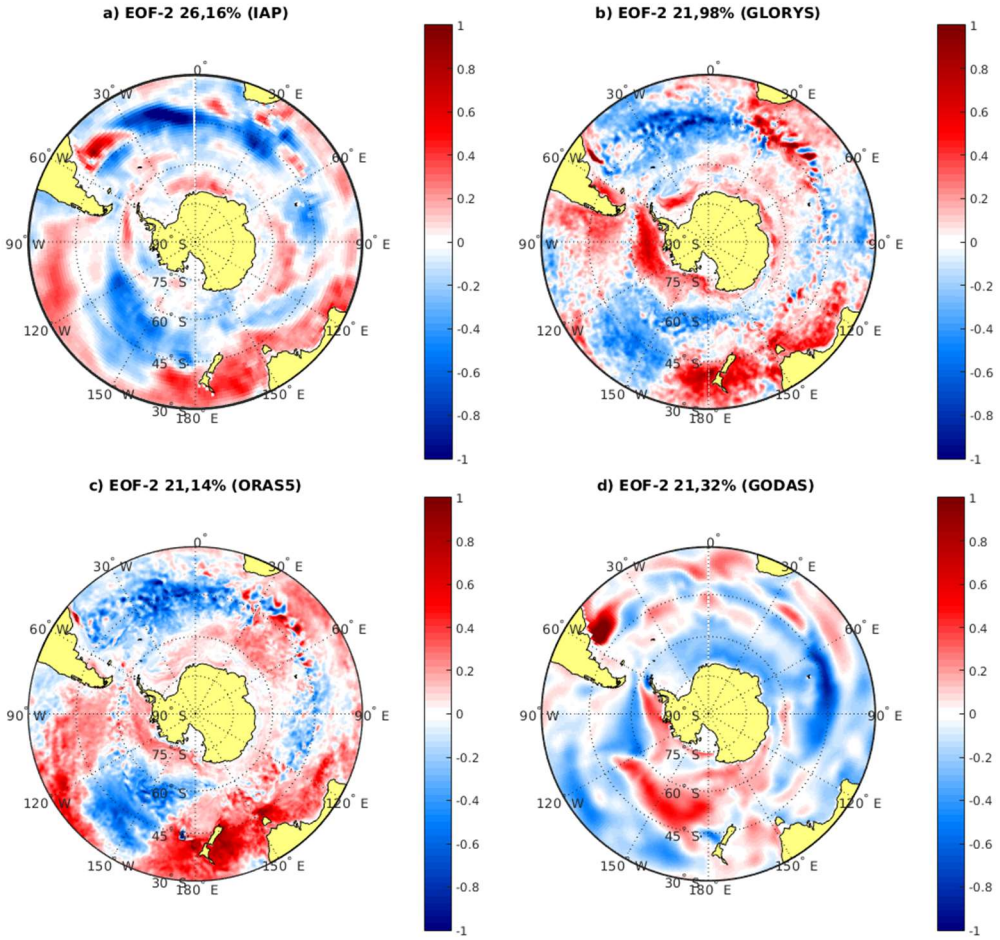

Figure 5: Second EOF for the IAP (a), GLORYS (b), ORAS5 (c) and GODAS (d). The values in the heading are the explained variance for each dataset.

A dipole is presented near the South American coast at 45ºS in the Atlantic Ocean by GODAS and IAP, but the same is not repeated for GLORYS and ORAS5. This difference is associated with the interpretation of oceanic eddies where the Brazil-Malvinas Confluence (BMC) is dominant. The BMC originates from the junction of Brazil and the Malvinas Current in the Southwest Atlantic, this meeting originates energetic eddies (Matano; Schlax; Chelton, 1993; Stramma & England, 1999; Imawaki *et al.*, 2013, to cite a few). As GODAS and IAP do not reproduce eddies processes that cause dispersion of heat content from the hot side to the cold side of the BMC resulting in misrepresented variability along the BMC.

3.3 Correlation with climate indexes

To verify the impact of the tropics on the oceanic heat content, the correlation between the OHC and ENSO is shown in Figure 3. The ENSO as discussed by Yuan (2004) in its positive phase causes a strengthened subtropical jet over the Pacific region and a weakened polar jet and

changes the position of the jet in the southernmost Atlantic portion. This enhances the OHC flux in the Pacific but reduces in the Atlantic. The ENSO (Fig. 6) and OHC are positively correlated in most of the southern Pacific (Balmaseda; Trenberth; Källén, 2013; Trenberth; Fasullo; Balmaseda, 2014), but the region is reduced in GODAS dataset. Negative correlations are dominant across in particular in Pacific Ocean mid-latitudes. Values in the South Atlantic do not exhibit a dominant pattern and may be more related to local features, that are highly correlated to SST (eg., Hall & Visbeck, 2002; Holland; Bitz; Hunke, 2005; Lovenduski & Gruber, 2005; Sengupta & England, 2006; Meredith *et al*., 2008). GLORYS, ORAS5, IAP and GODAS show the Antarctic dipole with a positive phase in the Pacific Ocean and a negative phase in the Atlantic Ocean, in the vicinity of the Antarctic peninsula (e.g. Meredith *et al*., 2008; Holland; Bitz; Hunke, 2005).

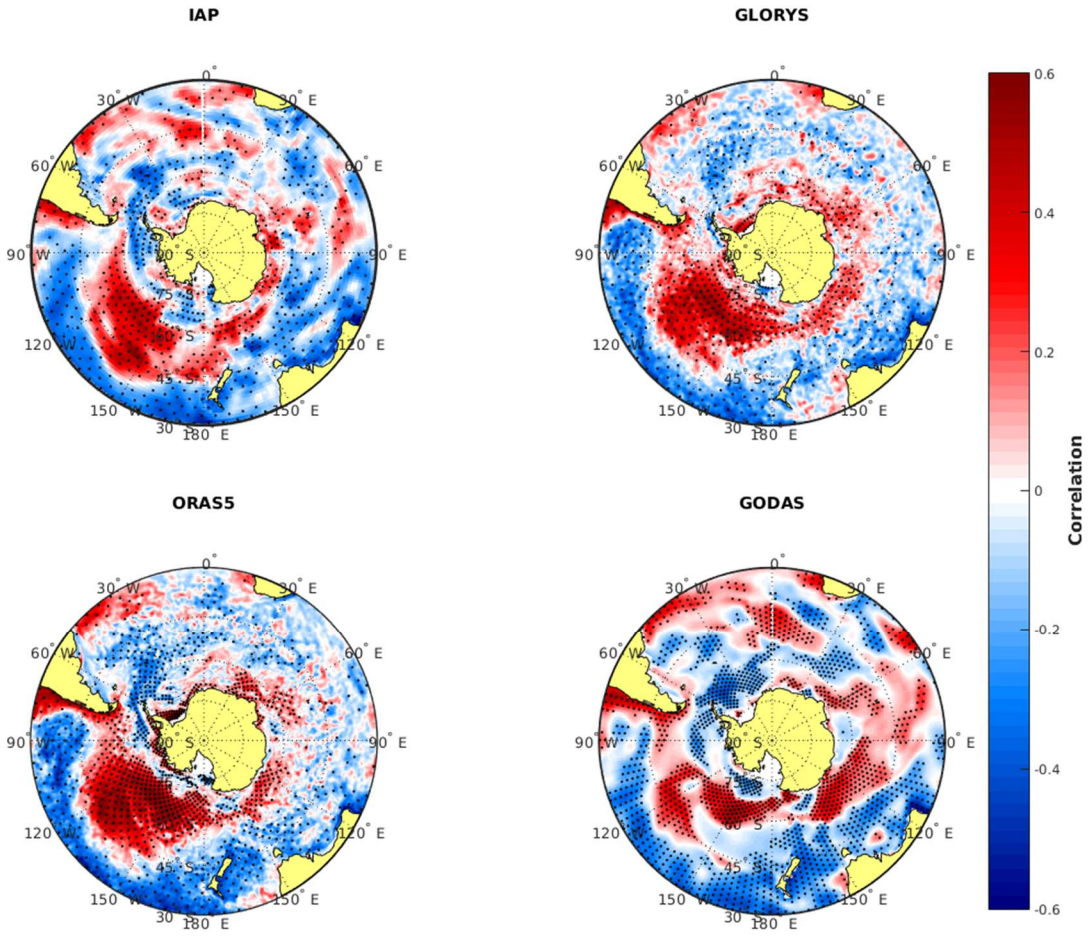

Figure 6: Correlation between the ENSO and the OHC. Dotted regions mean statistical significance of 95%.

The correlations of SAM with the OHC anomaly which are confined over small regions, have little significance in IAP and GODAS (Fig. 7). GLORYS and ORAS5 present a larger

region of significant negative correlation in the middle of the Pacific Ocean and positive in the Southwest Atlantic. The lower resolution of IAP and GODAS can be responsible for this lack of correlation, however, Screen *et al*. (2009) demonstrated that eddies only become relevant for inducing significant correlations between the SAM and OHC/SST, at annual lags with peak at 3 years. Despite the lower influence of horizontal resolution and eddies, a proper representation of vertical discretization is fundamental for representing processes on subsurface layers, which induce cold or warm biases leading to misrepresentation of temporal changes of OHC (Cheng & Zhu, 2014).

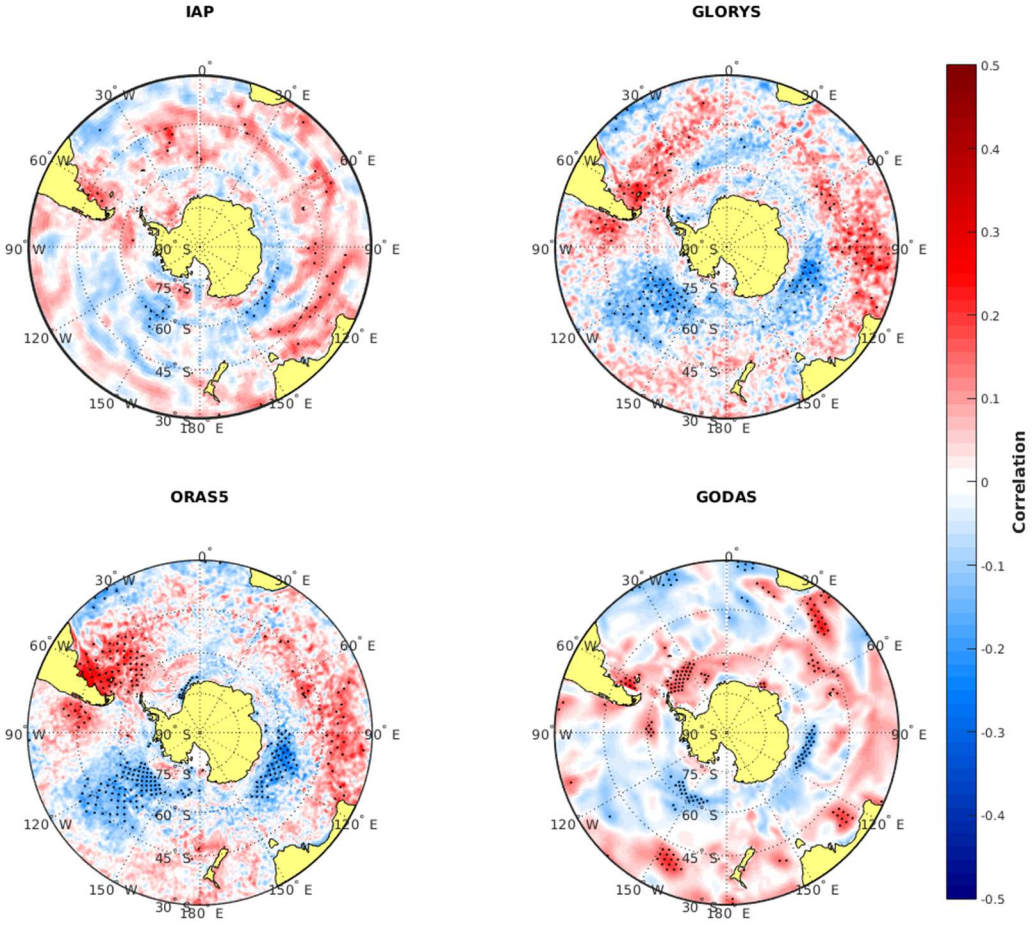

Figure 7: Correlation between the SAM and the OHC. Dotted regions mean statistical significance of 95%.

The correlation of OHC with SAM shown by GLORYS and ORAS5 is explained by SAM being linked to a positive westerly wind anomaly at approximately 55ºS and negative anomalies by about 35ºS. These wind anomalies generate an increase in upwelling in the Antarctic Polar Front and downwelling of the surface water in the Subantarctic Zone. This

pattern leads to positive SST anomaly in the Subtropical Zone and negative SST anomaly in the Antarctic Zone and Polar Frontal Zone (Londuski & Gruber, 2005). The correlation clearly shows the out-of-phase feature over South America coastal waters and the central Pacific. Increased OHC and higher SST in the later region have been linked to increased storminess over southern Brazil and contributed for the first observed Brazilian hurricane in 2004, namely Catarina (Pezza & Simmods, 2005; McTaggart-Cowan *et al*., 2006).

In the following it is analyzed the influence of SAM in the OHC but removing the ENSO signal according to the equation below (Zar, 1998; Saji & Yamagata, 2003; Hu & Duan, 2015):

$$r_{AB,C} = \frac{r_{AB} - r_{AC} r_{BC}}{\sqrt{(1 - r_{AC}^2)(1 - r_{BC}^2)}}$$

Where A is the OHC, B is the SAM index and C the ENSO index. r_{ij} is the correlation between the variables and $r_{AB,C}$ is the correlation between OHC and SAM removing the ENSO signal.

Figure 8 shows the individual correlation between the OHC and the SAM. It is very clear similarities among datasets showing higher values with positive correlations, along the Indian Ocean and South America coastal waters. Despite the important role of ENSO, the regional impact of the SAM should be considered in particular due to its influence on South Atlantic. This part of the SO is path to baroclinic atmospheric features that enhances frontal characteristics increasing continental precipitation, which is fundamental for agricultural and energy activities. It's important to notice that without the ENSO signal the SAM don't have more a significant correlation in the Pacific Ocean. This indicates that SAM acts as a regulator of the impacts of ENSO in the SO.

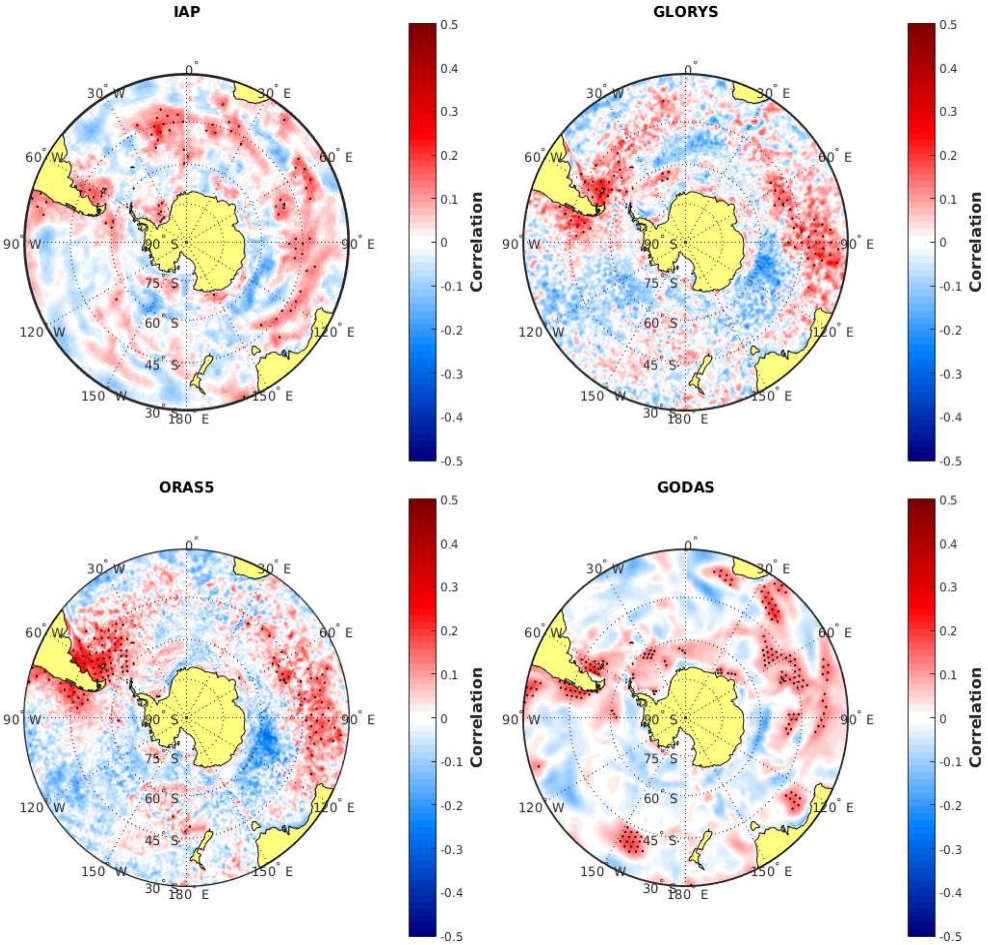

Figure 8: Correlation between the SAM and the OHC without ENSO signal. Dotted regions mean statistical significance of 95%.

3.4. OHC from the oceanic modelling experiments

Too analyze the GDFL-MOM025 and GFDL-MOM (here after just MOM025 and MOM) models representation of the OHC, was take an annual average of the GLORYS model (GLORYS-AM) to serve as a comparison with the models.

The GLORYS-AM trend (Figure 9c) north of 60ºS remains similar to the results previously found for the monthly average, with regions with significant positive trends in almost the entire portion north of 45ºS with values ranging from $1x10^8$ J/m^2 to the peak of approximately $2.5x10^8$ J/m^2 in the northern region of the CBM. South of 60°S different from the negative trend in almost the entire portion of the ocean near the Antarctic Continent previously presented by GLORYS, GLORYS-AM has almost no regions with significant negative trends and presents a range of positive trends from the Weddell Sea to the sea similar to the one presented by IAP earlier.

MOM025 and MOM (Figure 9 a, b) show trends with values lower than GLORYS-AM ranging between -1 and 1x10^8 J/m^2. MOM025 represents the positive range north of 45°S but in the Pacific Ocean where GLORYS-AM has a positive range that goes from 120°E to 90°W MOM025 has this range going up to approximately 130°W. MOM in turn, different from MOM025 and GLORYS-AM has fewer regions with significant trends. And few regions with positive trends north of 45°S, for example, in the Pacific Ocean between 120 and 90°W and in the Southwest Atlantic.

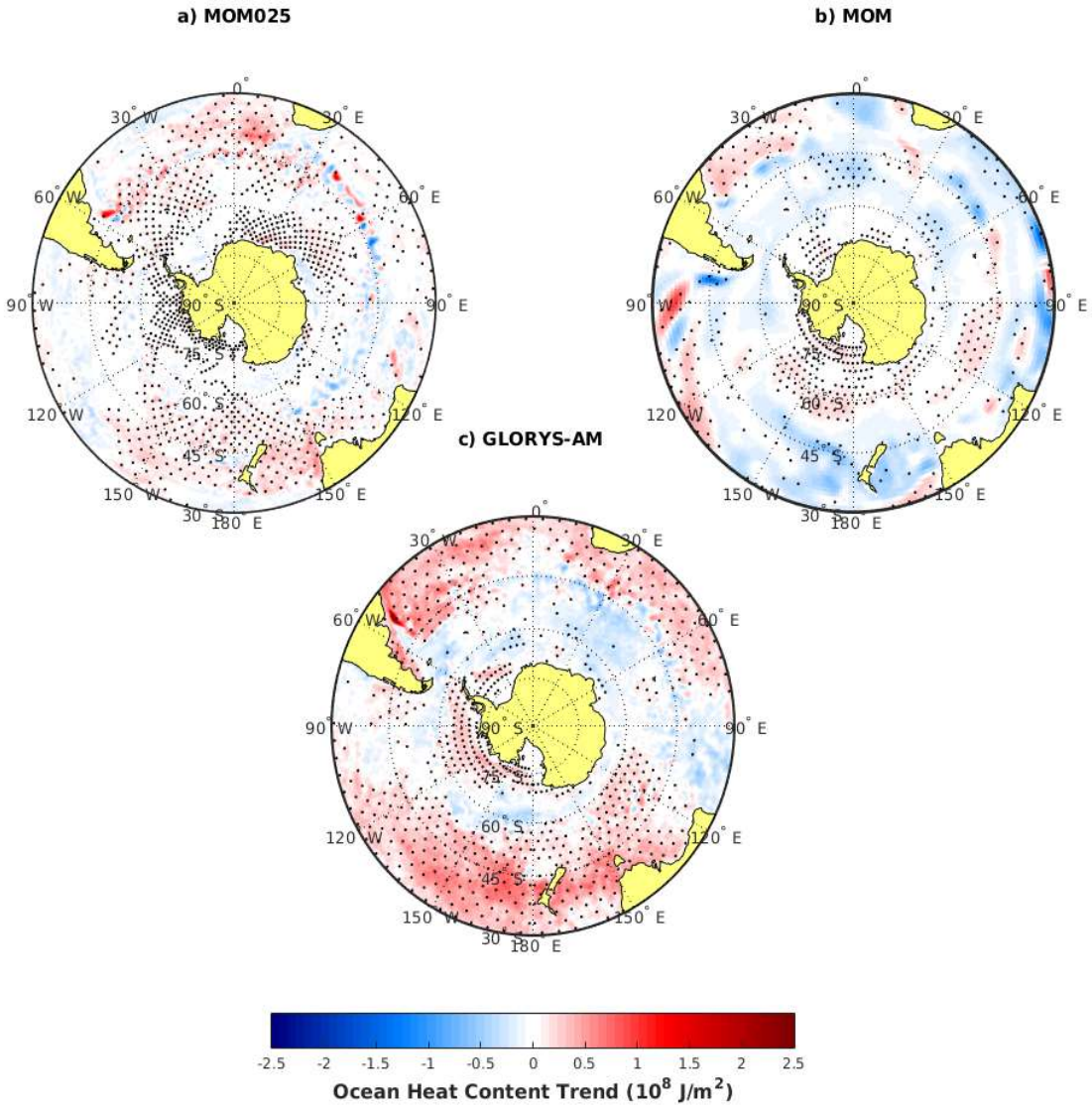

Figure 9: OHC trend for the MOM025 (a), MOM (b) and GLORYS-AM (c). Regions with statistical significance at 95% are dotted.

The first EOF (Figure 10) shows that the models fail to represent the characteristic variability mode of the first EOF the Antarctic Dipole. GLORYS-AM (Figure 10c) despite still

showing a negative region in the Pacific Ocean, different from the monthly data, does not present the characteristic positive region in the Atlantic Ocean that would configure the Antarctic Dipole. MOM025 despite showing a positive region in the Atlantic portion, in the Pacific Ocean it does not have the expected negative region for the first EOF. MOM in turn has negative values in most of the western portion of the Southern Ocean and positive in most of the eastern portion.

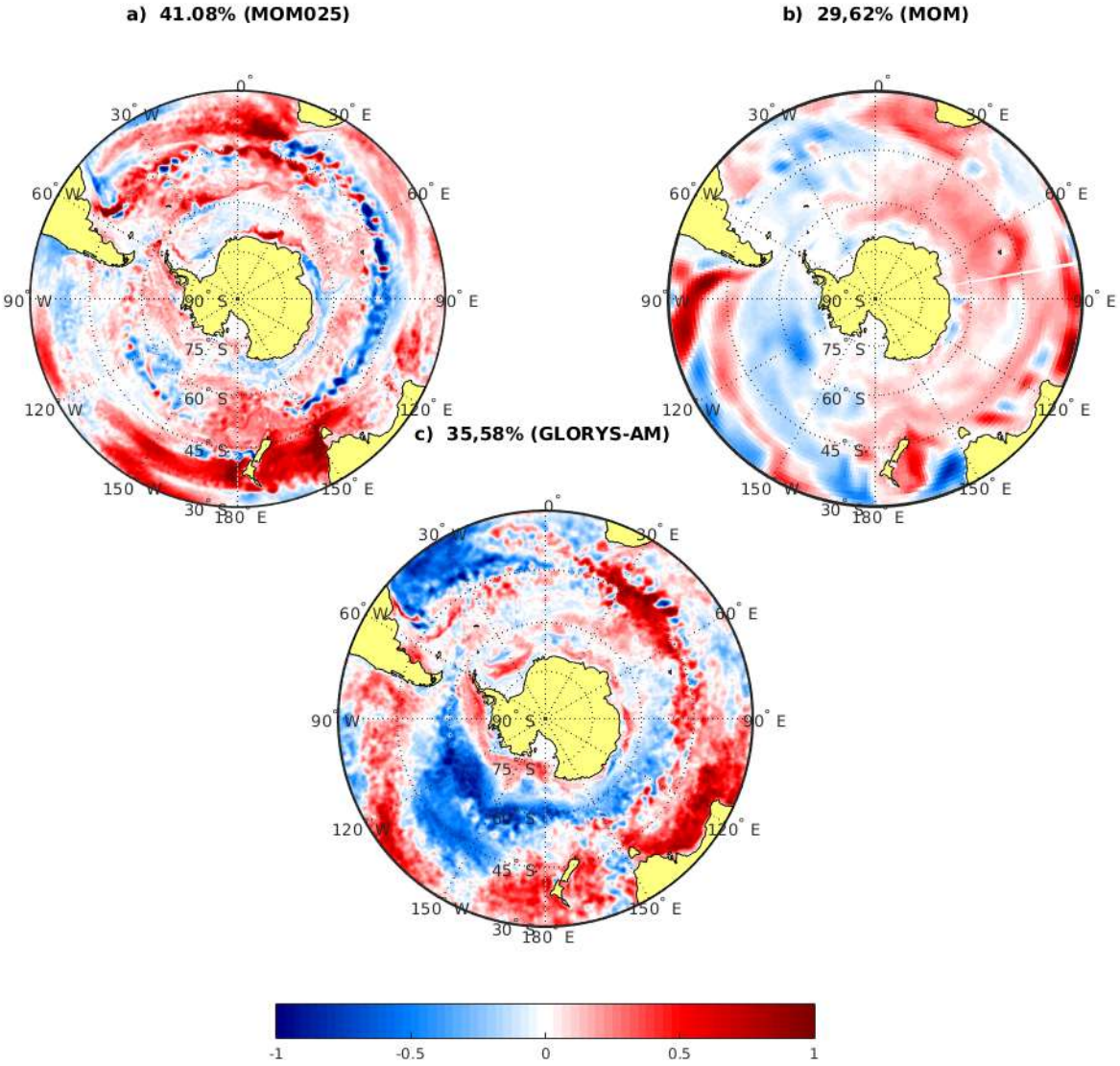

Figure 10: First EOF for the MOM025 (a), MOM (b) and GLORYS-AM (c). The values in the heading are the explained variance for each dataset. All the values have been normalized for a better comparison.

As discussed, previously, the first EOF of the OHC, is directly linked to the ENSO and has a high inverse correlation with it (Table 2). So, to elucidate why MOM025 and MOM cannot satisfactorily represent the 1st EOF of the OHC, we must analyze their relationship with ENSO (Figure 11). MOM025 disregards any direct relationship between the OHC and the ENSO, showing only a few points with significant correlations in the Pacific Ocean at 120°W and the Weddell Sea coast. MOM in turn presents a strong positive correlation in the western portions of the Pacific and Atlantic oceans between 45 and 60ºS, and further north between 45 and 30°S in the western portion of the Indian Ocean. GLORYS-AM presents an expected correlation between ENSO and OHC in the Pacific Ocean, but the significant area is more focused at 60°S while in monthly data this same one extended to 45°S. However, GLORYS-AM does not find a correlation between ENSO and the OHC in the Atlantic Ocean, which justifies the absence of the Antarctic Dipole in the 1st EOF.

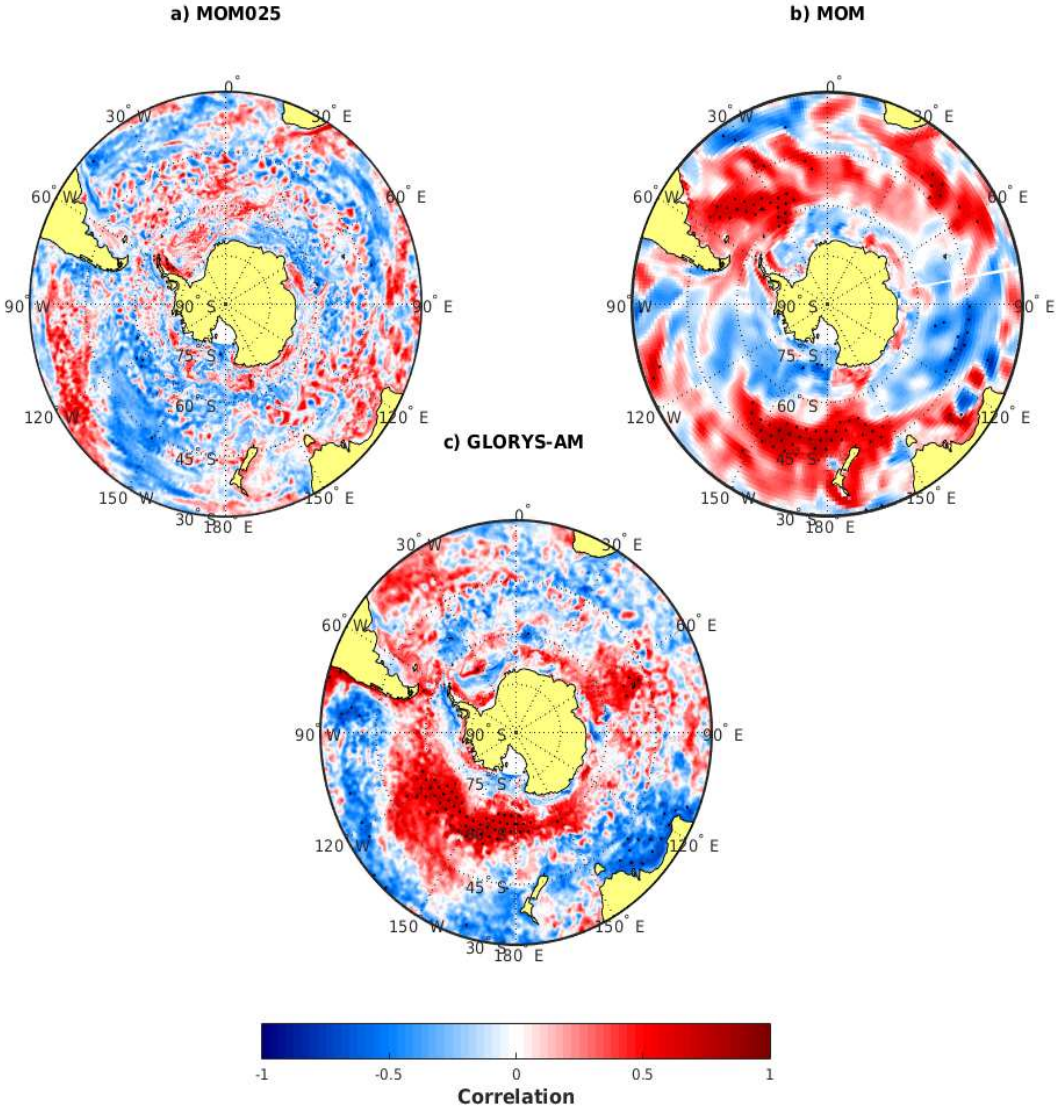

Figure 11: Correlation between the ENSO and the OHC for the MOM025 (a), MOM (b) and GLORYS-AM (c). Dotted regions mean statistical significance of 95%.

4. Conclusion

The reanalysis shows a good representation of the OHC in the first 300 meters, they have a similar trend and correlation with known climate variability modes. GODAS besides being the reanalysis with less resolution and lacking the capacity to resolve ocean eddies can in general represents a satisfactory OHC in the SO, but still, the results show the impact that an interpretation on the ocean eddies have in the OHC profiles. This became more obvious when seen the differences in the EOF's of the data sets, mostly on the second EOF. GLORYS and ORAS5 who have an eddy-permitting model show similar modes of variability, as also similar PCs, for the second EOF as also are the one who has a higher correlation with the SAM, this may be because SAM is directly associated with the changes in the Westerlys, and the impact of this in the ACC (Gillet & Thompson, 2003; Fyfe & Saenko, 2006, Fyfe *et al*., 2007), a very turbulent region where the ocean eddies have a huge impact in the heat distribution. Besides the Eddies, the reanalysis good representation of the OHC in the upper layers is most likely because of the remote sensing data taken in the SO, which leads to an increase in the input data in the models improving their capability in representing oceans variables highly correlated to the SST.

ENSO is the main climate variability module affecting the OHC and is responsible for generating the Antarctic Dipole presented in the first EOF. ENSO is also inversely linked to PC1 with a correlation extending to at least six months across all databases. The correlation of SAM with OHC is only represented by GLORYS and ORAS5 and presents an Antarctic Dipole with an opposite signal to ENSO. However, the removal of the ENSO signals in the correlation between SAM and OHC it ceases to have a significant role in the Pacific Ocean, finding that it acts only in the sense of weakening the impact of ENSO on the SO.

Both oceanic models analyzed fail to properly represent the OHC and its variability, this is due to the fact that they neglect the impact of ENSO on the SO. This raises the question of whether this would be a limitation of the MOM model, or the settings used by the CORE-II models. In conclusion, the GLORYS and ORAS5 reanalysis are able to represent the variability characteristics of OHC in the OS satisfactorily. GODAS has major limitations in the representation of the OHC and fails to represent the second EOF as well as the IAP highlighting the importance of eddies representation in the region.

The limitations presented by ocean models point us to a new question. How the other CORE-II models represent the OHC? considering that these models are used to forecast future

scenarios and a satisfactory representation of the OHC is of fundamental importance for this. More studies are necessary to understand this issue, since ocean models are still an important tool for a continuous study of the SO and to a better understanding of its impact on the global climate and its paper on the climate changes.

5. References

ABERNATHEY, R. P.; CEROVECKI, I.; HOLLAND, P.R.; NEWSOM, E.; MAZLOFF, M.; TALLEY, L.D. Water-mass transformation by sea ice in the upper branch of the Southern Ocean overturning. **Nat. Geosci.**, v. 9, p. 596-601, 2016.

ALMEIDA, L.; MAZLOFF, M. R.; MATA, M. M. The impact of Southern Ocean Ekman pumping, heat and freshwater flux variability on intermediate and mode water export in CMIP models: present and future scenarios. **Journal of Geophysical Research: Oceans**, v. 126, e2021JC017173, 2021. doi:10.1029/2021JC017173.

ARMOUR, K. C.; MARSHALL, J.; SCOTT, J. R.; DONOHOE, A.; NEWSOM, E. R. Southern Ocean warming delayed by circumpolar upwelling and equatorward transport. **Nat. Geosci.**, v. 9, p. 549-554, 2016.

ARMOUR, K. C.; BITZ, C. M. Observed and projected trends in Antarctic sea ice. **US CLIVAR Variations**, v. 13, n. 4, p. 13-19, 2015.

AUGER, M.; MORROW, R.; KESTENARE, E.; SALLÉE, J.-B.; COWLEY, R. Southern Ocean in-situ temperature trends over 25 years emerge from interannual variability. **Nat. Commun.**, v. 12, 2021. doi:10.1038/s41467-020-20781-1.

BALMASEDA, M. A.; TRENBERTH, K. E.; KÄLLÉN, E. Distinctive climate signals in reanalysis of global ocean heat content. **Geophys. Res. Lett.**, v. 40, p. 1754-1759, 2013. doi:10.1002/grl.50382.

BEHRINGER, D.; XUE, Y. Evaluation of the global ocean data assimilation system at NCEP: the Pacific Ocean. In: SYMPOSIUM ON INTEGRATED OBSERVING AND ASSIMILATION SYSTEMS FOR ATMOSPHERE, OCEAN, AND LAND SURFACE, 8, 2004, Seattle. **Proceedings…** Seattle: American Meteorological Society, 2004.

BRACEGIRDLE, T. J.; SHUCKBURGH, E.; SALLEE, J.-B.; WANG, Z.; MEIJERS, A. J. S.; BRUNEAU, N.; … WILCOX, L. J. Assessment of surface winds over the Atlantic, Indian, and Pacific Ocean sectors of the Southern Ocean in CMIP5 models: historical bias, forcing response, and state dependence. **J. Geophys. Res. Atmos.**, v. 118, p. 547-562, 2013. doi:10.1002/jgrd.50153.

CHENG, L.; ZHU, J. Uncertainties of the Ocean Heat content estimation induced by insufficient vertical resolution of historical ocean subsurface observations. **Journal of Atmospheric and Oceanic Technology**, v. 31, n. 6, p. 1383-1396, 2014.

CHENG, L.; TRENBERTH, K.; FASULLO, J.; BOYER, T.; ABRAHAM, J.; ZHU, J. Improved estimates of ocean heat content from 1960 to 2015. **Science Advances**, v. 3, e1601545, 2017.

DANABASOGLU, G.; YEAGER, S. G.; BAILEY, D.; BEHRENS, E.; BENTSEN, M.; BI, D.; … WANG, Q. North Atlantic simulations in Coordinated Ocean-ice Reference Experiments phase II (CORE-II). Part I: mean states. **Ocean Modelling**, v. 73, p. 76-107, 2014.

DEE, D. P.; UPPALA, S. M.; SIMMONS, A. J.; BERRISFORD, P.; POLI, P.; KOBAYASHI, S.; … VITART, F. The ERA-Interim reanalysis: configuration and performance of the data assimilation system. **Quarterly Journal of the Royal Meteorological Society**, v. 137, n. 656, p. 553-597, 2011. doi:10.1002/qj.828.

DELWORTH, T. L.; ROSATI, A.; ANDERSON, W.; ADCROFT, A. J.; BALAJI, V.; DELWORTH, R. B. L.; … ZHANG, R. Simulated climate and climate change in the GFDL CM2.5 high-resolution coupled climate model. **J. Climate**, v. 25, p. 2755-2781, 2012.

DUFOUR, C. O.; GRIFFIES, S. M.; SOUZA, G. F.; FRENGER, I.; MORRISON, A. K.; PALTER, J. B.; … SLATER, R. D. Role of mesoscale eddies in cross-frontal transport of heat and biogeochemical tracers in the Southern Ocean. **Journal of Physical Oceanography**, v. 45, n. 12, p. 3057-3081, 2015. doi:10.1175/JPO-D-14-0240.1.

EAYRS, C.; HOLLAND, D. M.; FRANCIS, D.; WAGNER, T. J. W.; KUMAR, R.; LI, X. Understanding the seasonal cycle of Antarctic Sea ice extent in the context of longer-term variability. **Reviews of Geophysics**, v. 57, p. 1037-1064, 2019. doi:10.1029/2018RG000631.

FAN, T.; DESER, C.; SCHNEIDER, D. P. Recent Antarctic Sea ice trends in the context of Southern Ocean surface climate variations since 1950. **Geophys. Res. Lett.**, v. 41, p. 2419-2426, 2014. doi:10.1002/2014GL059239.

FARNETI, R.; DOWNES, S. M.; GRIFFIES, S. M.; MARSLAND, S. J.; BEHRENS, E.; BENTSEN, M.; … YEAGER, S. G. An assessment of Antarctic Circumpolar Current and Southern Ocean meridional overturning circulation during 1958-2007 in a suite of interannual CORE-II simulations. **Ocean Modelling**, v. 93, p. 84-120, 2015. doi:10.1016/j.ocemod.2015.07.009.

FERRY, N.; PARENT, L.; GARRIC, G.; BARNIER, B.; JOURDAIN, N. Mercator global Eddy permitting ocean reanalysis GLORYS1V1: description and results. **Mercator-Ocean Q Newslett.**, v. 36, p. 15-27, 2010.

FRÖLICHER, T. L.; SARMIENTO, J. L.; PAYNTER, D. J., DUNNE, J. P., KRASTING, J. P., & WINTON, M. Dominance of the Southern Ocean in anthropogenic carbon and heat uptake in CMIP5 models. **Journal of Climate**, v. 28, n. 2, p. 862-886, 2015. doi:10.1175/jcli-d-14-00117.1.

FYFE, J. C.; SAENKO, O. A. Simulated changes in the extratropical Southern Hemisphere winds and currents. **Geophys. Res. Lett.**, v. 33, L06701, 2006. doi:10.1029/2005GL025332.

FYFE, J. C.; SAENKO, O. A.; ZICKFELD, K.; EBY, M.; WEAVER, A. J. 2007: The role of poleward-intensifying winds on Southern Ocean warming. **J. Climate**, v. 20, p. 5391-5400, 2007. doi:10.1175/2007JCLI1764.1.

GARABATO, A. C. N.; JULLION, L.; STEVENS, D. P.; HEYWOOD, K. J.; KING, B. A. variability of subantarctic mode water and Antarctic intermediate water in the drake passage during the late-twentieth and early-twenty-first centuries. **Journal of Climate**, v. 22, n. 13, p. 3661-3688, 2009. doi:10.1175/2009jcli2621.1.

GILLETT, N. P.; THOMPSON, D. W. J. Simulation of recent southern hemisphere climate change. **Science**, v. 302, n. 5643, p. 273-275, 2003. doi:10.1126/science.1087440.

GRIFFIES, S.; GNANADESIKAN, A.; DIXON, K.; DUNNE, J.; GERDES, R.; HARRISON, M.; … ZHANG, R. Formulation of an ocean model for global climate simulations. **Ocean Science**, v. 1, 2005. doi:10.5194/osd-2-165-2005.

HALL, A.; VISBECK, M. Synchronous variability in the Southern Hemisphere atmosphere, sea ice, and ocean resulting from the Annular Mode. **J. Clim.**, v. 15, p. 3043-3057, 2002.

HOLLAND, M. M.; BITZ, C. M.; HUNKE, E. C. Mechanisms forcing an Antarctic dipole in simulated sea ice and surface ocean conditions, **Journal of Climate**, v. 18, n. 12, p. 2052-2066, 2005.

HU, J.; DUAN, A. Relative contributions of the Tibetan Plateau thermal forcing and the Indian Ocean Sea surface temperature basin mode to the interannual variability of the East Asian summer monsoon. **Clim. Dyn.**, v. 45**,** p. 2697-2711, 2015. doi:10.1007/s00382-015-2503-7.

IMAWAKI, S.; BOWER, A. S.; BEAL, L. M.; QIU, B. Western boundary currents, in ocean circulation and climate: a 21-century perspective. **International Geophysics**, v. 103, n. 13, p. 305-338, 2013. doi:10.1016/B978-0-12-391851-2.00013-1.

JUSTINO, F.; SETZER, A.; BRACEGIRDLE, T. J.; MENDES, D.; GRIMM, A.; DECHICHE, G.; SCHAEFER, C.E.G.R. Harmonic analysis of climatological temperature over Antarctica: present day and greenhouse warming perspectives. **Int. J. Climatol.**, v. 31, p. 514-530, 2011. doi:10.1002/joc.2090.

JUSTINO, F.; SILVA, A. S.; PEREIRA, M. P.; STORDAL, F.; LINDEMANN, D.; KUCHARSKI, F. The large-scale climate in response to the retreat of the west Antarctic ice sheet. **Journal of Climate**, v. 28, n. 2, p. 637-650, 2015. doi:10.1175/jcli-d-14-00284.1.

JUSTINO, F.; WILSON, A. B.; BROMWICH, D. H.; AVILA, A.; BAI, L.-S.; WANG, S.-H. Northern Hemisphere extratropical turbulent heat fluxes in ASRv2 and global reanalysis. **J. Climate**, v. 32, p. 2145-2166, 2019. doi:10.1175/JCLI-D-18-0535.1.

KEPPLER, L.; LANDSCHÜTZER, P. Regional wind variability modulates the Southern Ocean carbon sink. **Sci. Rep.**, v. 9, p. 7384, 2019. doi:10.1038/s41598-019-43826-y.

LANDSCHÜTZER, P.; GRUBER, N.; HAUMANN, F. A.; RÖDENBECK, C.; BAKKER, D. C. E.; VAN HEUVEN, S.; … WANNINKHOF, R. The reinvigoration of the Southern Ocean carbon sink. **Science**, v. 349, n. 6253, p. 1221-1224, 2015. doi:10.1126/science.aab2620.

LARGE, W. G.; YEAGER, S. G. The global climatology of an interannually varying air-sea flux data set. **Climate Dyn.**, v. 33, p. 341-364, 2009.

LECOMTE, O.; GOOSSE, H.; FICHEFET, T.; DE LAVERGNE, C.; BARTHÉLEMY, A.; ZUNZ, V. Vertical Ocean heat redistribution sustaining sea-ice concentration trends in the Ross Sea. **Nature Communications**, v. 8, n. 1, p. 258, 2017. doi:10.1038/s41467-017-00347-4.

LOVENDUSKI, N. S.; GRUBER, N. Impact of the Southern annular mode on Southern Ocean circulation and biology. **Geophys. Res. Lett.**, v. 32, L11603, 2005. doi:10.1029/2005GL022727.

LUMPKIN, R.; SPEER, K. Global Ocean meridional overturning. **J. Phys. Oceanogr.**, v. 37, p. 2550-2562, 2007.

MARINOV, I.; GNANADESIKAN, A.; TOGGWEILER, J. R.; SARMIENTO, J. L. The Southern Ocean biogeochemical divide. **Nature**, v. 441, p. 964-967, 2006.

MARSHALL, J.; SPEER, K. Closure of the meridional overturning circulation through Southern Ocean upwelling. **Nature Geosci.**, v. 5, p. 171-180, 2012. doi:10.1038/ngeo1391.

MARTÍNEZ-MORENO, J.; HOGG, A. M.; ENGLAND, M. H.; CONSTANTINOU, N. C.; KISS, A. E.; MORRISON, A. K. Global changes in oceanic mesoscale currents over the satellite altimetry record. **Nat. Clim. Change**, v. 11, p. 397-403, 2021. doi:10.1038/s41558-021-01006-9.

MARTINSON, D. G. Evolution of the Southern Ocean winter mixed layer and sea ice: open ocean deep water formation and ventilation. **Journal of Geophysical Research**, v. 95, n. C7, 1990. doi:10.1029/JC095iC07p11641.

MATANO, R. P.; SCHLAX, M. G.; CHELTON, D. B. Seasonal variability in the southwestern Atlantic. **J. Geophys. Res.**, v. 98, n. C10, p. 18.027-18.035, 1993. doi:10.1029/93JC01602.

McCARTNEY, M. S. Subantarctic mode water. In: ANGEL, M. **A voyage of discovery**: George Deacon 70th Anniversary. Pergamon, 1977. p. 103-119.

McCARTNEY, M. S. The subtropical recirculation of mode waters. **Journal of Marine Research**, v. 40, p. 427-464, 1982.

McDOUGALL, T. J.; BARKER, P. M. **Getting started with TEOS-10 and the Gibbs Seawater (GSW)**: oceanographic toolbox. SCOR/IAPSO WG127, 2011. 28 p.

McTAGGART-COWAN, R.; BOSART, L. F.; DAVIS, C. A.; ATALLAH, E. H.; GYAKUM, J. R.; EMANUEL, K. A. Analysis of Hurricane Catarina (2004). **Monthly Weather Review**, v. 134, n. 11, p. 3029-3053, 2006.

MEREDITH, M. P.; MURPHY, E. J.; HAWKER, E. J.; KING, J. C.; WALLACE, M. I. On the interannual variability of ocean temperatures around South Georgia, Southern Ocean: forcing by El Niño/Southern Oscillation and the Southern Annular Mode. **Deep Sea Research Part II: Topical Studies in Oceanography**, v. 55, n. 18-19, p. 2007-2022, 2008. doi:10.1016/j.dsr2.2008.05.020.

MEYSSIGNAC, B.; BOYER, T.; ZHAO, Z.; HAKUBA, M. Z.; LANDERER, F. W.; STAMMER, D.; … ZILBERMAN, N. Measuring global ocean heat content to estimate the earth energy imbalance. **Frontiers in Marine Science**, v. 6, 2019. doi:10.3389/fmars.2019.00432.

PELLICHERO, V.; SALLÉE, J.-B.; CHAPMAN, C. C.; DOWNES, S. M. The Southern Ocean meridional overturning in the sea-ice sector is driven by freshwater fluxes. **Nat. Commun.**, v. 9, n. 1789, 2018. doi:10.1038/s41467-018-04101-2.

PEZZA, A. B.; SIMMONDS. I. The first South Atlantic hurricane: unprecedented blocking, low shear and climate change. **Geophysical Research Letters**, v. 32, n. 15, 2005.

PEZZI, L.P.; SOUZA, R. B.; SANTINI, M. F.; MILLER, A. J.; CARVALHO, J.; PARISE, C. K.; … RUBERT, J. Oceanic eddy-induced modifications to air–sea heat and CO_2 fluxes in the Brazil-Malvinas Confluence. **Sci. Rep.**, v. 11, 10648, 2021. doi:10.1038/s41598-021-89985-9.

RHEIN, M.; RINTOUL, S. R.; AOKI, S. Observations: ocean. In: CLIMATE Change 2013. **The physical science basis**. Contribution of working group I to the fifth assessment report of the intergovernmental panel on climate change. Cambridge, NY: Cambridge University Press, 2013.

RINTOUL, S. R. The global influence of localized dynamics in the Southern Ocean. **Nature**, v. 558, p. 209-218, 2018. doi:10.1038/s41586-018-0182-3.

SABINE, C. L.; FEELY, R. A.; GRUBER, N.; KEY, R. M.; LEE, K.; BULLISTER, J. L.; … RIOS, A. F. The oceanic sink for anthropogenic CO2. **Science**, v. 305, n. 5682, p. 367-371, 2004. doi:10.1126/science.1097403.

SAJI, N. H.; YAMAGATA, T. Possible impacts of Indian Ocean dipole mode events on global climate. **Clim. Res.**, v. 25, n. 2, p. 151-169, 2003.

SALLÉE, J.-B. Southern Ocean warming. **Oceanography**, v. 31, n. 2, 2018. doi:10.5670/oceanog.2018.215.

SALLÉE, J.-B.; SHUCKBURGH, E.; BRUNEAU, N.; MEIJERS, A. J. S.; BRACEGIRDLE, T. J.; WANG, Z.; ROY, T. Assessment of Southern Ocean water mass circulation and characteristics in CMIP5 models: historical bias and forcing response. **J. Geophys. Res. Oceans**, v. 118, p. 1830-1844, 2013. doi:10.1002/jgrc.20135.

SARMIENTO, J. L.; GRUBER, N.; BRZEZINSKI, M. A.; DUNNE, J. P. High-latitude controls of thermocline nutrients and low latitude biological productivity. **Nature**, v. 427, p. 56-60, 2004.

SCHMIDTKO, S.; HEYWOOD, K. J.; THOMPSON, A. F.; AOKI, S. Multidecadal warming of Antarctic waters. **Science**, v. 346, n. 6214, p. 1227-1,231, 2014. doi:10.1126/science.1256117.

SCHNEIDER, W.; FUKASAWA, M.; UCHIDA, H.; KAWANO, T.; KANEKO, I.; FUENZALIDA, R. Observed property changes in eastern South Pacific Antarctic Intermediate Water. **Geophys. Res. Lett.**, v. 32, L14602, 2005. doi:10.1029/2005GL022801.

SCHNEIDER, D. P.; REUSCH, D. B. Antarctic and Southern Ocean Surface Temperatures in CMIP5 Models in the Context of the Surface Energy Budget. **Journal of Climate**, v. 29, n. 5, p. 1689-1716, 2016.

SCHUCKMANN, K.; PALMER, M.; TRENBERTH, K. E.; CAZENAVE, A.; CHAMBERS, D.; CHAMPOLLION, N.; … WILD, M. An imperative to monitor Earth's energy imbalance. **Nature Clim. Change**, v. 6, p. 138-144, 2016. doi:10.1038/nclimate2876.

SCREEN, J. A.; GILLETT, N. P.; STEVENS, D. P.; MARSHALL, G. J.; ROSCOE, H. K. The role of eddies in the Southern Ocean temperature response to the Southern annular mode. **Journal of Climate**, v. 22, n. 3, p. 806-818, 2009.

SENGUPTA, A.; ENGLAND, M. H. Coupled ocean-atmosphere-ice response to variations in the Southern annular mode. **Journal of Climate**, v. 19, p. 4457-4486, 2006.

SILVANO, A. Changes in the Southern Ocean. **Nat. Geosci.**, v. 13, p. 4-5, 2020. doi: 10.1038/s41561-019-0516-2.

SLOYAN, B. M.; RINTOUL, S. R. The Southern Ocean limb of the global deep overturning circulation. **J. Phys. Oceanogr.**, v. 31, p. 143-173, 2001.

SOUZA, J. M. A. C.; COUTO, P.; SOUTELINO, R.; ROUGHAN, M. Evaluation of four global ocean reanalysis products for New Zealand waters: a guide for regional ocean modelling. **New Zealand Journal of Marine and Freshwater Research**, v. 55, n. 1, p. 132-155, 2021. doi:10.1080/00288330.2020.1713179.

STEPHENSON, G. R.; GILLE, S. T.; SPRINTALL, J. Seasonal variability of upper ocean heat content in drake passage. **J. Geophys. Res.**, v. 117, C04019, 2012. doi:10.1029/2011JC007772.

STRAMMA, L.; ENGLAND, M. On the water masses and mean circulation of the South Atlantic Ocean. **J. Geophys. Res.**, v. 104, n. C9, p. 20.863-20.883, 1999. doi:10.1029/1999JC900139.

TRENBERTH, K. E.; FASULLO, J. T.; BALMASEDA, M. A. Earth's energy imbalance. **J. Clim.**, v. 27, p. 3129-3144, 2014. doi:10.1175/JCLI-D-13-00294.

UPPALA, S. M.; DEE, D. P.; KOBAYASHI, S.; SIMMONS, A. J. Evolution of reanalysis at ECMWF. In: WCRP International Conference on Reanalysis, 3, 2008, Tokyo, Japan. **Proceedings…** Tokyo, Japan, 2008.

VAUGHAN, D. G.; COMISO, J. C.; ALLISON, I.; CARRASCO, J.; KASER, G.; KWOK, R.; … REN, J. Observations: cryosphere. In: CLIMATE Change 2013. **The physical science basis**. Contribution of working group I to the fifth assessment report of the intergovernmental panel on climate change. Cambridge, NY: Cambridge University Press, 2013. p. 317-382.

WANG, G.; DOMMENGET, D. The leading modes of decadal SST variability in the Southern Ocean in CMIP5 simulations. **Climate Dynamics**, v. 47, n. 5-6, 1775-1792, 2015. doi:10.1007/s00382-015-2932-3.

WANG, G.; CHENG, L.; ABRAHAM, J.; CHONGYIN, L. Consensuses and discrepancies of basin-scale ocean heat content changes in different ocean analyses. **Climate Dynamics**, v. 50, p. 2471-2487, 2018. doi:10.1007/s00382-017-3751-5.

WATSON, A. J.; NAVEIRA GARABATO, A. C. The role of Southern Ocean mixing and upwelling in glacial-interglacial atmospheric CO_2 change. **Tellus B**, v. 58, p. 73-87, 2006. doi:10.1111/j.1600-0889.2005.00167.x.

YUAN, X. ENSO-related impacts on Antarctic Sea ice: a synthesis of phenomenon and mechanisms. **Antarctic Science**, v. 16, n. 4, p. 415-425, 2004. doi:10.1017/S0954102004002238.

ZAR, J. **Biostatistical analysis**. 4th ed. Boston: Pearson Education, 1998.

ZUO, H.; BALMASEDA, M. A.; TIETSCHE, S.; MOGENSEN, K.; MAYER, M. The ECMWF operational ensemble reanalysis–analysis system for ocean and sea ice: a description of the system and assessment. **Ocean Sci.**, v. 15, p. 779-808, 2019. doi:10.5194/os-15-779-2019.

2. CONCLUSÃO

Como foi possível observar pelos artigos 1 e 2, as reanálises GLORYS e ORAS5 apresentam uma satisfatória representação da temperatura da superfície do mar (TSM). Ambas têm padrões similares e apresentam um aquecimento/resfriamento ao norte/sul de 45°S. GODAS, por sua vez, apresenta tendências similares a ambas, porém com valores mais intensos e com mais regiões significativas de resfriamento. A possível causa deste resfriamento mais intenso deve-se à falta de um modelo de gelo em GODAS. Provavelmente, parte ou toda a perda de calor vai para a mudança de temperatura da água e não para a formação de gelo, fazendo com que ele tenha um resfriamento muito mais intenso que GLORYS ou ORAS5. Para ser possível confirmar essa suposição seria necessário fazer um teste rodando um modelo de gelo acoplado e outro sem para verificar se isso causaria essa diferença nas tendências de temperatura; mas isso está fora do escopo deste trabalho.

A CCO, assim como a TSM, é bem representada pelas reanálises, em especial GLORYS e ORAS5. Todas as reanálises apresentam um claro aumento na CCO, porém GODAS apresenta uma tendência inferior às outras duas. Todas as reanálises apresentam um intervalor entre 2000 e 2011 com anomalias negativas de OHC. Esse resultado foi encontrado por outros autores, mostrando a capacidade das reanálises em reproduzir padrões e tendências conhecidos do OA. O ENSO é o principal módulo de variabilidade climática a impactar todas as reanálises. Entretanto, somente GLORYS e ORAS5 apresentam um ciclo de 5-7 anos no seu primeiro módulo de variabilidade semelhante ao ENSO, mostrando que GODAS subestima o impacto da ENSO no OA.

A SAM aparece como um segundo módulo de variabilidade a impactar o CCO nas reanálises GLORYS e ORAS5; e GODAS descarta qualquer relação entre SAM e CCO em até seis meses de lag. O impacto da SAM no CCO já é conhecido pela comunidade cientifica, contudo foi possível perceber que, ao remover o sinal do ENSO na SAM, ela perde sua característica de dipolo. De fato, com a ausência do ENSO, a SAM passa a ter somente relações significativas positivas com a CCO na porção mais sul da costa do Continente Americano e no Oceano Índico. Essa mudança nas correlações pode ser interpretada como a SAM somente agindo no Oceano Pacífico simplesmente como um contraponto ao impacto da ENSO no mesmo. Tais resultados não são mostrados por GODAS, o que demonstra grande limitação em representar a CCO no AO. Isso se deve principalmente ao fato de ela não ter uma representação dos vórtices oceânicos. É evidente que, apesar de GODAS apresentar uma primeira EOF similar

às outras duas reanálises, ela falha em representar a segunda EOF que está diretamente ligada a vórtices ciclônicos.

Os dois experimentos rodados nos parâmetros do CORE-II falham em representar a CCO e sua variabilidade no OA. Isto ocorre em virtude de os dois modelos ignorarem o impacto do ENSO no OA. Tal falha pressupõe um questionamento: isso se deve a uma limitação do modelo MOM utilizado pelos dois experimentos ou aos parâmetros usados pelos modelos do CORE-II?

A principal diferença entre as reanálises aparece quando se analisa a densidade, mais especificamente, a salinidade. Ao contrário da TSM que, além de dados *in situ*, tem o aporte de anos de dados de sensoriamento remoto, fazendo com que as reanálises apresentem valores e variabilidades similares; a salinidade tem uma limitação maior de dados, principalmente no OA, no qual os dados *in situ* são coletados majoritariamente nos meses de verão. GLORYS e ORAS5 que, até o momento, eram as duas reanálises com resultados mais próximos diferem completamente quando se trata de salinidade. Das três reanálises, ORAS5 é o que mais difere das outras reanálises e de outros trabalhos por apresentar uma tendência negativa de salinidade na maior parte do OA. Essa tendência possivelmente deve-se ao fato de ORAS5 ser restringido pela sua climatologia pela técnica *nudging.* Porém, como já foi discutido, os dados de salinidade do OA são retirados majoritariamente nos meses de verão, nos quais o OA apresenta sua menor salinidade e isto pode ser o responsável pelo erro.

Em resumo, é possível perceber que, em relação à TSM, as reanálises oceânicas apresentam uma boa descrição da variável tanto em seu comportamento médio como em sua tendência. Isso ocorre, possivelmente, devido aos dados derivados de sensoriamento remoto. Apesar de GODAS, em um primeiro momento, ter resultados similares em alguns pontos a GLORYS e ORAS5, a CCO tem sua representação limitada, pois descarta os vórtices oceânicos. A salinidade aparece aqui como o próximo e principal desafio a ser enfrentado pela comunidade científica, uma vez que não existe um consenso em valores e tendências nem entre bancos de dados coletados *in situ*. Ainda assim, as reanálises oceânicas permanecem como uma importante ferramenta para o estudo do Oceano Austral. Uma contínua observação destas reanálises se faz necessária para que se possam localizar os próximos passos para melhorá-las.